PHOSPHORUS IN THE DENSE INTERSTELLAR MEDIUM

B. E. TURNER
National Radio Astronomy Observatory,[1] Charlottesville

T. TSUJI
Tokyo Astronomical Observatory

J. BALLY
AT&T Bell Laboratories, Holendel

M. GUELIN
IRAM, Grenoble

AND

J. CERNICHARO
IRAM, Granada

ABSTRACT

We have made an observational study of interstellar (and circumstellar) phosphorus chemistry by means of (1) a survey of PN in energetic star-forming regions (several new detections); (2) a search for PN in cold cloud cores; and (3) a search for HPO, HCP, and PH_3 in interstellar and circumstellar sources. Our results are consistent with the ion-molecule models of phosphorus chemistry developed by Thorne and coworkers and by Millar and coworkers and imply large depletion factors for P in dense clouds: $\sim 10^3$ in warm star-forming cores and more than 10^4 in cold cloud cores. We have made thermochemical equilibrium models for the P chemistry in C-rich and O-rich environments, and find that HCP contains all the phosphorus in the C-rich case. Our search for HCP in IRC 10216 yields an upper limit which, taken together with our recent detection of CP, implies significant depletion of HCP onto grains, according to our LVG analysis for an expanding circumstellar envelope. We summarize depletion factors for first- and second-row elements in diffuse and dense interstellar clouds, and propose an overall picture of circumstellar and interstellar grain and gas-phase processes to explain the depletions of N, O, C, S, Si, P, and in particular the high depletions of Si and P.

Subject headings: interstellar: matter — interstellar: molecules

I. INTRODUCTION

Compared with the first-row chemical elements (C, N, O), the second-row elements (Si, P, S?) are generally believed to be highly depleted in dense molecular clouds. Si, in particular, is assumed to be locked into grains. Although phosphorus is not depleted in warm diffuse clouds, it is already depleted by a factor of 3 in cooler diffuse clouds ($A_v \lesssim 2$ mag) (Dufton, Keenan, and Hibbert 1986).

The second-row elements pose important questions for astrochemistry: (1) Are they systematically more depleted in dense clouds than the first-row elements? (2) Can we identify differences in their chemistry relative to that of first-row elements that suggest that grain chemistry is important? These questions are relevant to understanding not only the composition of grains in dense clouds but also their survival under a variety of energetic conditions such as violent shocks or even severe heating in massive star-forming regions and near supernovae. Thus these questions are relevant to understanding the life-cycles of grains. As Seab (1987) has discussed, there are problems in understanding how grains maintain their observed abundances, given current assessments of their formation rates in evolved stellar envelopes and their destruction rates by supernovae. The implication is that much of the grain mass in the interstellar medium (ISM) is formed by accretion (but not

condensation), a process directly related to the depletion of the elements. Because of their relatively high cosmic abundances and their refractory nature, the elements of the second and third rows are the important ones in studying the growth, structure, and evolution of interstellar grains. They may be studied in dense interstellar clouds only by the observation of their molecular species. To interpret such observations, one must understand the gas-phase chemistry of these elements, in order to determine in what form they are adsorbed on or desorbed from grains. For example, the observation (Turner and Steimle 1985) that $MgO/SiO \lesssim 10^{-3}(Mg/Si)$ could be explained either by the much stronger (crystalline) binding of MgO than that of the (amorphous) SiO or by a relative inability of gaseous Mg to form molecules (in particular MgO) under interstellar conditions.

Progress toward understanding the gas-phase chemistry of P has been made by Thorne, Anicich, and Huntress (1983) and Thorne et al. (1984), and recently of Si by Herbst et al. (1989). P chemistry is quite different from that of the analogous first-row element N (§ V). In their initial model, Thorne et al. (1984) predicted that PO would be the most abundant interstellar P compound (although it was subsequently not detected by Matthews, Feldman, and Bernath 1987), and failed to predict a significant abundance for PN (although subsequently detected by Turner and Bally 1987 and Ziurys 1987). To explain the observed PN, so far the only detected interstellar P compound, Millar, Bennett, and Herbst (1987) added the reaction $PO + N \rightarrow PN + O$ to the Thorne et al. (1984) scheme. If

TURNER, TSUJI, BALLY, GUELIN, AND CERNICHARO

this reaction has no activation barrier, then PN is predicted to be the most abundant P compound, followed by HPO (at 15 times smaller abundance) and all other P species well below currently detectable levels. In the discovery papers (Turner and Bally 1987; Ziurys 1987), PN was detected in the energetic star-forming regions in Ori(KL), W51M, and Sgr B2. The abundance ratio was found to be $PN/P \sim 5 \times 10^{-4}$, rather lower than the SiO/Si ratio of $\sim 6 \times 10^{-3}$ in Ori(KL) (Turner and Steimle 1985). These results do not allow a choice between several possibilities, e.g., (1) that PN forms via $PO + N \rightarrow PN + O$ as a result of temperatures high enough to overcome an activation barrier and (2) that grains could be disrupted in star-forming regions and preferentially release PN (and SiO) as products of the disruption.

In the present paper we report results of a survey of PN in additional star-forming regions, of a highly sensitive search for PN in cold dark clouds, and of searches for HPO, PH_3, and HCP as tests of the gas phase models of Thorne et al. (1984), and Millar, Bennett, and Herbst (1987). In addition to the interstellar problem, we consider P chemistry under thermochemical equilibrium conditions in circumstellar envelopes (CSEs), and report results of a search for HCP in IRC 10216 as well as calculations which predict it to be the most abundant P compound in C-rich CSEs. Finally, we present a picture of grain evolution in both diffuse and dense interstellar regions, which is consistent with observed depletions of first- and second-row elements.

II. OBSERVATIONS

Most of the observations were made at the NRAO 12 m telescope. The survey of PN at 234.93569 GHz ($J = 5-4$) in warm clouds was made in 1987 May; the survey of PN at 93.97978 GHz ($J = 2-1$) in cold clouds was made in 1987 June; and the searches for HPO, PH_3, and HCP in the 1.3 mm region were made in 1987 November and 1988 April.

At 1.3 mm, the dual-channel cooled Schottky mixer-receiver was used in double-sideband (DSB) operation, accepting orthogonal linear polarizations. The beamwidth varies from 39″ at 199 GHz to 28″ at 280 GHz. The telescope was position-switched 30′ in azimuth. Spectral resolution was 1 MHz.

At 94 GHz the telescope was equipped with the dual-channel SIS junction receiver tuned for single-sideband (SSB) operation. SSB noise temperature was typically 135 K. Orthogonal linear polarizations were accepted by the two channels. The beamwidth was 69″. For the cold clouds, spectral resolution was 30 kHz (0.096 km s^{-1}) in one spectrometer and 25 kHz (0.080 km s^{-1}) in a "spectrum-expanded" 100 kHz filter bank. The telescope was "absolute"-position–switched to positions selected well outside the extended clouds. For the warmer sources (DR 21OH, M17), spectral resolution was 100 and 250 kHz, respectively, and the telescope was position-switched 30′ in azimuth.

Temperature scales for 12 m observations are $T_R^* = \eta_f \eta_c T_B$, where η_f is the geometric beam dilution of the source, T_B the brightness temperature, and η_c the fractional efficiency in the forward hemisphere of the main beam. At 94 GHz $\eta_c = 0.79$, and η_c varied from 0.58 to 0.36 between 199 and 280 GHz. The telescope was not equipped with its present, shaped, subreflector.

Observations of HCP in IRC 10216 were also made at 160 and 240 GHz with the IRAM 30 m telescope. Those at 160 GHz are part of a spectral scan of IRC 10216 carried out in the 2 mm spectral region (cf. Cernicharo and Guelin 1987b). At 160 GHz $T_A^* \equiv \eta_f \eta_c \eta_{fss} T_B \approx 0.6\eta_f T_B$ (where η_{fss} is the forward spillover and scattering efficiency, and the beamwidth $\theta_B = 17″$. At 240 GHz, $T_A^* \approx 0.5\eta_f T_B$ and $\theta_B = 12″$.

III. PN SURVEYS AND ABUNDANCES

a) PN at 94 GHz ($J = 2-1$) in Cold Dense Clouds

We define a cold core as one with kinetic temperature $T_k < 20$ K. PN was not detected in its $J = 2-1$ transition at 93.97978 GHz in any of the nine cold cloud cores searched. Upper limits and other particulars are given in Table 1.

Several of the cold-core sources (TMC-1, TMC-2, L1544, L183, L134, B335) appear to have properties similar to those of TMC-1. They appear to be quiescent objects not occurring in the immediate vicinity of star formation. They are among a large number of such objects appearing in the recent compendium of cold dark cores by Benson and Myers (1989). Values of T_k are always ~ 10 K, as shown by observations of both CO (Myers, Linke, and Benson 1983) and NH_3 (Benson and Myers 1989). Densities in several cases (TMC-1, L183, L134, B335) are established to be between 3×10^4 and 10^5 cm^{-3} (cf. Avery, MacLeod, and Broton 1982; Swade 1987; Swade and Schloerb 1987). Such densities likely apply in all objects studied here, judging from the NH_3 studies of Benson and Myers (1989).

The other three cold cores listed in Table 1 (L1689N, ρ Oph A, ρ Oph B) all occur in the star-forming ρ Oph complex, and

TABLE 1
SURVEY OF PN IN COLD CLOUDS AT 94 GHz ($J = 2-1$)

Source	R.A.(1950)	Decl.(1950)	Resolution (kHz)	Velocity Range (km s^{-1})	T_k (K)	T_R^* (mK)[a]
TMC-1	04^{h}38^{m}38$\overset{s}{.}$0	25°35′45″	30	5.9 ± 6.1	10	<20
TMC(C_3H_2)	04 38 12.5	25 43 54	30	5.9 ± 6.1	9.6[b]	<35
L1544	05 01 15.0	25 07 00	30	7.2 ± 6.1	9.8[b]	<70
L134	15 51 00.0	−04 26 51	30	3.0 ± 6.1	9.0[b]	<50
L183	15 51 28.0	−02 41 30	30	3.0 ± 6.1	9.5[b]	<50
ρ Oph A	16 23 25.5	−24 15 49	30	3.3 ± 6.1	35–45	<50
ρ Oph B1	16 24 08.9	−24 22 49	30	3.3 ± 6.1	~18[c]	<50
L1689N	16 29 20.9	−24 22 13	30	4.0 ± 6.1	~15[d]	<50
B335	19 34 34.7	07 27 20	30	8.0 ± 6.1	9.9[b]	<40

[a] At 94 GHz, $T_B = T_R^*/\eta_c = 1.26T_R^*$.
[b] From Benson and Myers 1989.
[c] From Loren and Wootten 1986.
[d] From Wootten and Loren 1987.

thus may encounter less quiescent conditions than the TMC-1 type objects. L1689N (Wootten and Loren 1987) consists of a dense cold clump ($n \sim 10^6$ cm^{-3}, $T_k \sim 15 \pm 5$ K), an adjacent IR source (IRAS 16293−422) in a distinct warmed clump 0.07 pc to the west, and a bipolar mass outflow probably associated with the IR object. Like TMC-1, the L1689N core is rich in complex C molecules and has a high dust column depth. The objects ρ Oph A and B1 are two of three dense, cold star-forming cores studied by Loren and Wootten (1986). The conditions (T_k, n) are 35 K, 1.5×10^5 cm^{-3} for A, and ~ 18 K, 8.7×10^4 cm^{-3} for B1. The B1 core appears not to contain an embedded star but to be heated somewhat above the equilibrium cold cloud temperature of 10 K by a passing shock. The elevated temperature of core A is due to its proximity to nearby massive stars, such as the BZ 4 H II region.

We have analyzed our negative PN results with a large velocity gradient (LVG) radiative transfer model, using collision cross sections for HC$_3$N, whose dipole and quadrupole moments are similar to those of PN. Eighteen rotational levels of PN are included, and an isothermal, homogeneous, spherical cloud is assumed. We take $T_k = 10$ K and n ranging from 5×10^3 to 1.5×10^5 cm^{-3}, depending on the source. The results are collected in Table 2. The derived normalized fractional abundance, X', depends strongly on the adopted density but rather weakly on the value of T_k in the range 10–20 K. The actual fractional abundance is $X = X'(dv/dR)$. Because the velocity gradient dv/dR is rather poorly known for most sources, we derive the PN fractional abundance as $X = N(PN)/N(H_2)$, with $N(PN) = X'n\,\Delta v$ and $N(H_2)$ as derived from values of $N(NH_3)$ by Benson and Myers (1989), assuming a constant value of $X(NH_3)$ for all clouds, and the value $N(H_2) = 1.0 \times 10^{22}$ cm^{-2} for TMC-1 (Cernicharo and Guelin 1987a). Line widths (Δv) are adopted from various other molecules and listed in Table 2. For comparison, we include in Table 2 values of $X = X'(dv/dR)$, using values of $dv/dR = 1.0$ and 2.5 km s^{-1} pc^{-1} for L134 and L183 as established by Wootten, Snell, and Evans (1980), and adopting an average value of 1.7 km s^{-1} pc^{-1} for the other sources. In general the

two methods agree satisfactorily (within a factor of 3). The exception is L134.

The results (Table 2) establish $X(PN)$ less than a few times 10^{-12} for TMC-1 and TMC-1 (C$_3$H$_2$), and less than a few times 10^{-11} for the other seven cold clouds. By contrast, $X(PN) \sim 2 \times 10^{-10}$ in the three star-forming sources Ori(KL), W51M, and Sgr B2 and, as we shall see, in M17SW, DR 21OH, and NGC 7538 as well. Such a difference far exceeds the uncertainties in determining $X(PN)$ and points to a different chemistry for PN in cold and in warm sources. We discuss this in § V.

b) PN in Warm Molecular Clouds

The original detection of PN was made only in the most energetic star-forming regions, Ori(KL), W51M, and Sgr B2. Thus it was possible to argue that PN formed as a result of grain mantle disruption (Turner and Bally 1987) or as a result of high-temperature gas-phase reactions involving P. To decide between these and other possibilities, it is necessary to investigate a broader selection of energetic star-forming regions, since such regions are quite varied.

Table 3 summarizes the observational results. Five regions, all containing star formation, were searched in the $J = 2$–1 transition. Six objects, including three star-forming regions, one supernova remnant, and two CSEs, were searched in the $J = 5$–4 transition.

New detections of PN at 94 GHz were made in the star-forming regions M17SW and DR 21OH. These are shown in Figure 1. A tentative detection was made toward NGC 7538. Line widths are ~ 5 km s^{-1} for both DR 21OH and M17SW, quite typical of other complex molecules seen toward these sources. In the previously detected sources Ori(KL), W51M, and Sgr B2, PN line widths were also typical of those of other species arising in the core regions, although only Ori(KL) exhibits broader core line widths characteristic of energetic phenomena. The tentative PN feature in NGC 7538 has width ~ 14 km s^{-1}, the same as the CO width (Scoville et al. 1986).

To investigate why PN should be found in these particular

TABLE 2
PN Abundance Limits in Cold Cloud Cores

Source	T_B (mK)[a]	n (cm^{-3})	Δv (km s^{-1})	X'	$X'(dv/dR)$[b]	log $N(NH_3)$	$X = \dfrac{N(PN)^c}{N(H_2)^c}$
TMC-1	<25	6(4)[d]	0.20[e]	<5(−13)	<8.6(−13)	15.1	<1.8(−12)
TMC-1 (C$_3$H$_2$)	<44	6(4)	0.4[e]	<9(−13)	<1.5(−12)	15.1	<6.3(−12)
L1544	<89	5(3)	0.39[e]	<6(−11)	<1.0(−10)	15.0	<4.3(−11)
L134	<63	1.3(5)[d]	0.72[e]	<4(−13)	<4.0(−13)	14.6	<3.4(−11)
L183	<83	1.3(4)[d]	0.25[e]	<1.5(−11)	<3.7(−11)	14.7	<3.7(−11)
ρ Oph A	<63	1.5(5)[g]	...	<4(−13)	<6.9(−13)	...	...
ρ Oph B1	<63	8.7(4)[g]	1.33[h]	<6(−13)	<1.0(−12)	...	...
L1689N	<63	3(4)[i]	0.6[h]	<1.8(−12)	<3.1(−12)	...	...
B335	<50	6.3(3)[d]	0.38[e]	<3(−11)	<5.2(−11)	14.9	<3.3(−11)

[a] $T_B = 1.26T_R^*$ at 94 GHz; η_f is assumed unity in all cases.

[b] dv/dR is taken as 1.72 km s^{-1} pc^{-1} (TMC-1) in all cases except L134 and L183, where values of 1.0 and 2.5 are established by Wootten, Snell, and Evans 1980.

[c] $N(H_2)$ derived from $N(NH_3)$. See text.

[d] Benson and Myers 1989.

[e] Matthews, Bell, and Feldman 1988 using C$_2$S.

[f] Wootten, Snell, and Evans 1980, using H$_2$CO.

[g] Loren and Wooten 1986.

[h] Madden et al. 1989, using C$_3$H$_2$.

[i] Wootten and Loren 1987; there is a cold clump with $n \sim 10^6$ cm^{-3} embedded with the overall core

TABLE 3

SURVEY OF PN IN WARM STAR-FORMING SOURCES

Source	R.A.(1950)	Decl.(1950)	Resolution (kHz)	Velocity Range (km s^{-1})	T_k (K)	T_R^* (mK)
A. $J = 2–1$ at 93.979 GHz						
OMC-N	05^{h}32^{m}51^{s}0	−05°20′21″	30	9.0 ± 6.1	30	≤50
Ori B	05 39 14.4	−01 57 00	100	9.0 ± 41	45	20^a
NGC 2264	06 38 25.0	09 32 28	30	8.5 ± 6.1	25	50^b
M17SW	18 17 27.0	−16 13 55	250	19.4 ± 102	50	31
DR 21OH	20 37 15.0	42 12 00	250	−3.0 ± 102	35	31
B. $J = 5–4$ at 234.936 GHz^c						
NGC 2071	05^{h}44^{m}30^{s}6	00°20′42″	1000	−5.0 ± 409	>30	<80
IC 443C	06 14 44.0	22 22 54	1000	9.0 ± 409	50	<80
IRC 10216	09 45 14.8	13 30 40	2000	−26.0 ± 818	30–600	<200
CIT 6	10 13 12.0	30 49 24	1000	−1.5 ± 409	30–600	<100
W51–IRS2	19 21 22.4	14 25 13	1000	57.0 ± 409	150	≤80
NGC 7538	23 11 36.7	61 11 48	1000	−59.0 ± 409	100	∼100

^{a} Possible detection at 9.0 km s^{-1}, line width = 1.3 km s^{-1} (4 channels).
^{b} Possible detection at 8.5 km s^{-1}, line width = 1.2 km s^{-1} (12 channels).
^{c} At 235 GHz, $T_B = T_R^*/\eta_c \sim 2.13 T_R^*$.

sources but not in the other warm molecular clouds surveyed, we need to summarize what is known of the physical conditions in the surveyed objects.

M17 is a well-known H II region, excited by nine O5 stars, which has formed a "blister" at the edge of the molecular cloud. The morphology is similar to that of Orion, except that it is viewed edge-on. The dense M17SW molecular core is at the H II–molecular cloud interface. There are several 10 μm IR sources at this position, and extended luminous 100 μm flux which shows the gas and dust temperatures to be in the 50–120 K range at the M17SW core. The ultracompact H II region at the M17SW core indicates the presence of a strong shock there. Our observed position is that of the peak C_3H_2 emission (Gerin et al. 1987) and also of the peak $C^{34}S$ emission (Mundy et al. 1986). This position is 1′ south of the ultracompact H II

region and strongest 10 μm sources (Mundy 1984) and 1′ north of the Kleinman–Wright IR source. In a detailed model of the M17SW interface region, Stutzki et al. (1988) find three components: (1) warm clump cores ($T_k = 50$ K, $n > 5 \times 10^4$ cm^{-3}, $N \sim 5 \times 10^{23}$ cm^{-2}); (2) hot clump envelopes, heated by UV from the H II region ($T_k = 200$ K, $n \sim 3 \times 10^4$ cm^{-3}, $N \sim 3 \times 10^{22}$ cm^{-2}); (3) cool, ambient gas ($T_k = 25$ K, $n \sim 3 \times 10^4$ cm^{-3}, $N \lesssim 10^{22}$ cm^{-2}). Clump cores and heated envelopes together have an estimated beam filling factor $\eta_f \sim 0.7$, while the warm cores themselves have $\eta_f \sim 0.2$. Massi, Churchwell, and Felli (1988) find six clumps of NH_3 emission with the VLA, each of size ∼0.05 pc, $N \sim 7 \times 10^{23}$ cm^{-2}, and $n \sim 5 \times 10^6$ cm^{-3}. Only one clump lies within our observing beam. This study appears to register only a fraction of the gas (Wilson and Walmsley 1989), most of which might occur at only modestly lower densities, since the available single-dish studies suggest that the fraction of the flux seen with the VLA is small (Snell et al. 1984). For conditions relevant to PN, the best guess is structures between 0.05 pc and a size of ∼0.4 pc, as suggested by the IR results.

DR 21OH is heated by the embedded OH maser protostellar object and possibly by W75S–IRS 1 lying 1′ to the west. IR results (Harvey et al. 1986) indicate a dust temperature of 35–40 K. The DR 21OH region is a massive star-forming one, somewhat less evolved than Ori(KL) or M17SW. Based on observations of the (7, 7) level of NH_3, the DR 21OH star-forming object likely has a core/halo structure, the halo having $T_k \sim 35$ K, $n \gtrsim 10^5$ cm^{-3} and the core having $T_k \sim 150$ K, $n \gtrsim 10^6$ cm^{-3} (Mangum, Wootten, and Mundy 1989).

NGC 2264 is a region of massive star formation, as indicated by the presence of OH and H_2O masers, which also contains cold, dense molecular cores as shown by the presence of DCO^+ (Wootten, Loren, and Snell 1982). The dense core we have observed has $T_k = 25$ K, $n = 2 \times 10^5$ cm^{-3} (Wootten, Loren, and Snell 1982; Linke and Goldsmith 1980).

Ori B (NGC 2024) is a region undergoing low-mass but perhaps not massive star formation, as suggested by lack of OH masers and by far-IR results (Thronson et al. 1984). The central region is a dense molecular cloud lying in front of the H II region, with little or no material behind the H II region, which is excited by a B0 zero-age main-sequence (ZAMS) star.
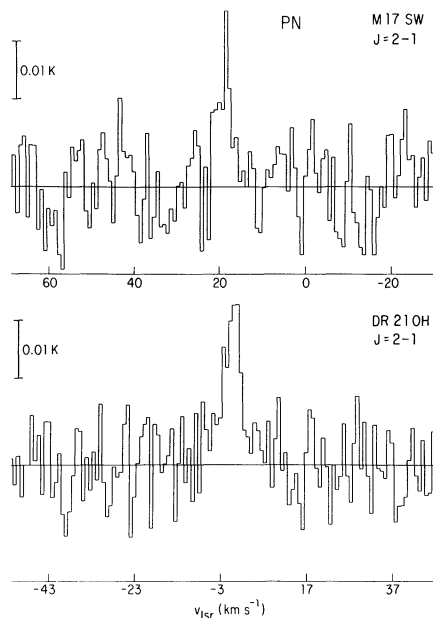

FIG. 1.—New detections of PN in star-forming regions

Dust temperature is ~ 45 K, and densities are a few times 10^5 cm^{-3}, representative of dense clumps within a more tenuous gas. The two bright near-IR objects IRS 1 and IRS 2 contribute less than 50% of the total far-IR luminosity. IRS 2 is embedded in the dense molecular cloud, whose properties appear similar to those of the ambient "ridge" cloud in Orion.

Ori(1, 4) or OMC-N, is a region in the OMC where the gas is more quiescent than at KL, $T_k \sim 30$ K, and $n \sim 10^6$ cm^{-3} (Wilson and Walmsley 1989). The region is an excellent candidate for formation of massive stars, and contains two clumps each of size 0.05 pc and of order 10 $M_\odot$ (Harris et al. 1983). OMC-N may result at least partly from compression caused by the H II region Orion A. Certain species such as N_2H^+, C_3H_2, and C_2H are very abundant in OMC-N, but HCO^+ is conspicuously unenhanced.

W51–IRS 2, which lies 2.2 pc from W51M, appears to comprise a hot ($T_k \sim 150$ K), dense ($n \gtrsim 10^7$ cm^{-3}) disk of order 100–200 $M_\odot$ surrounding a very luminous and massive protostellar object (Bally et al. 1987). These properties are consistent with those derived from high-excitation (7, 7) NH_3 lines (Mauersberger, Henkel, and Wilson 1987).

NGC 7538 contains a cluster of three IR objects $2'$ southeast of the visible H II region. A strong bipolar flow is centered on IRS 1, apparently channeled by a compact disk of size $22'' \times 7''$ and mass ~ 500 $M_\odot$, in which $T_k \sim 100$ K, $n \sim 2 \times 10^6$ cm^{-3} (Scoville et al. 1986). The bipolar flow is extended over $\sim 1\!'.5$, or 1.2 pc. Over the inner $30''$–$45''$ the flow characteristics are $T_k \sim 35$ K, $n \sim 10^4$–10^5 cm^{-3} (Campbell and Thompson 1984). The entire region around IRS 1–3 is undergoing compression by the advancing H II region.

NGC 2071 (distance 500 pc) is a reflection nebula located in the northern part of the OMC complex. A strong bipolar flow is centered near three IR objects which also display continuum emission at 6 cm wavelength (Persson et al. 1981; Snell and Bally 1986). The bipolar flow extends over 0.9×0.2 pc (Snell et al. 1984). A high-density "extended" ridge oriented roughly perpendicular to the flow has been reported by Lichten (1982) and Bally (1982), the latter estimating $T_k \sim 30$ K and $n \sim 10^5$ cm^{-3} from CS observations with a $100''$ beam. With a $30''$ beam Takano et al. (1984) find a smaller disk but do not report values of T_k and n, which may be expected to be somewhat larger. The smaller disk is not evident in interferometric maps of CO by Scoville et al. (1986).

IC 443C is one of several dense molecular clumps in the southeast rim of the supernova remnant shell IC 443. Our position (Table 3) is close to both the center of highest velocity shocked gas ($06^h14^m41\!^s.9$, $22°22'40''$) and to a second position having intense molecular emission but with only moderate velocities ($06^h14^m44\!^s.1$, $22°23'30''$) as determined by White et al. (1987). Physical conditions are poorly known in clump C, but Ziurys, Snell, and Dickman (1989) find $T_k \sim 50$ K, $n \sim 6 \times 10^5$ cm^{-3} in two other clumps (B and G). Clump sizes are also uncertain, but appear to be $\gtrsim 30''$.

Because the detailed structure of star-forming regions is poorly known in most instances, determination of molecular fractional abundances is highly uncertain compared with those determined in cold cloud cores. Even where such structure is well studied, as with interferometers, the different physical regimes (cores versus surrounding gas) may have very different physical characteristics, and assumptions must be made as to where a particular molecular species, such as PN, occurs. The dominant uncertainty in our analysis is, however, the beam dilution, or equivalently the brightness temperature of the

molecular lines. Compared with this uncertainty, those of T_k and n are minor.

Whether by selection effect or for more fundamental reasons, star-forming clumps in energetic warm cloud cores seem to have a characteristic size of 0.02–0.05 pc, with $n \sim 2 \times 10^6$ cm^{-3} and $T_k \sim 100$–250 K. These properties are observed interferometrically in a variety of species, including hot NH_3 [Ori(KL), W31C, W51M, NGC 7538; Mauersberger et al. 1986], warm NH_3 (M17SW: Massi, Churchwell, and Felli 1988; OMC-N: Harris et al. 1983), HCO^+ and HCN (NGC 7538: Pratap, Batrla, and Snyder 1990), and continuum (DR 21OH: Mangum, Wootten, and Mundy 1988; Ori B: Mezger et al. 1988). The number of such clumps varies considerably, however, from one in Ori(KL) to ~ 60 HCN clumps in NGC 7538. The observed values of T_R^* for PN vary by only a factor of 2, in both $J = 2$–1 and $J = 5$–4 transitions, among the six objects in which PN is now observed. Distances to these objects vary by a factor of 24. Therefore, PN is unlikely to be confined to the immediate vicinity of the small clumps, since more clumps than appear to be observed would have to occur within the observing beam for the more distant sources. More likely, PN seems to arise over a larger star-forming region, at least for the more distant objects such as Sgr B2 and W51M.

Because of these uncertainties, we have analyzed the PN results for more than one set of physical conditions for the newly detected sources M17SW and NGC 7538, representing the extreme case of PN confinement to 0.05 pc clumps and the more likely case of more extended regions as suggested by IR observations. Since velocity gradients are poorly known in star-forming regions, we derive PN fractional abundances from the column density $N(\mathrm{PN}) = X'n\Delta v$, and $N(H_2)$, the latter being derived by several methods and given in Table 4. The results are given in Table 5.

We have reanalyzed the PN results obtained in the original studies of PN (Turner and Bally 1987; Ziurys 1987); they are given in Table 5 also. Turner and Bally obtained $X(\mathrm{PN}) = 2.5 \times 10^{-10}$, 10^{-11}, and 1.7×10^{-12} for Ori(KL), W51M, and Sgr B2, respectively. Of these, Ori(KL) is the best studied of any star-forming region ($T_k = 140$ K, $n = 10^6$ cm^{-3}), and the value $X = 2.5 \times 10^{-10}$ is probably quite reliable. Note that the present value of X for DR 21OH is very similar, and that DR 21OH is also well understood. For W51M, Turner and Bally (1987) adopted a source size of $20''$ (based on rotationally excited CH results), but the canonical clump size of 0.05 pc, as derived from hot NH_3 (Mauersberger et al. 1986) is equally likely. In the latter case, with $T_k = 50$ K, $n = 10^6$ cm^{-3}, we obtain $X \sim 2 \times 10^{-8}$. For Sgr B2, Turner and Bally assumed that the PN source filled the $69''$ beam, but a more likely size is $\sim 30''$, the half-intensity size of the 53 μm distribution found by Harvey, Campbell, and Hoffman (1977). In this case, with $T_k = 50$ K, $X(\mathrm{PN})$ should be scaled up to 5×10^{-11}. An extreme case corresponds to PN confined near the compact H II regions near the "main" position of Sgr B2, of size $\sim 7\!''.5$. Then X scales up to 8×10^{-10}, comparable to the value found for Ori(KL). However, Mauersberger et al. (1986) argue that hot NH_3 is present over a large volume in Sgr B2, so that the intermediate value $X(\mathrm{PN}) \sim 5 \times 10^{-11}$ seems most likely.

With the exception of the 0.05 pc clump case for W51M, which clearly seems too extreme, we conclude from Table 5 that $X(\mathrm{PN})$ lies in the range 10^{-12} to 10^{-9}, with a median value 3.5×10^{-11} but with a "most likely" value of $\sim 2 \times 10^{-10}$ as applies to Ori(KL) and DR 21OH.

There is little indication as to what physical conditions cor-

TABLE 4

PHYSICAL CONDITIONS IN STAR-FORMING REGIONS SEARCHED FOR PN

Source	Distance (kpc)	Core Size (arcsec)	Density (cm^{-3})	T_k (K)	Column Density (cm^{-2})	Notes
OMC-N	0.5	25	10^6	30	1.8×10^{23}	1
NGC 2071	0.5	~80	$>10^5$	30	6×10^{22}	2
Ori B	0.415	8	10^6	45	$\sim 3 \times 10^{23}$	3
NGC 2264	0.8–2.8	46?	2×10^5	25	2×10^{23}?	4
IC 443	0.55–2.0	≥ 30	6×10^5	50	2.6×10^{23}	5
M17SW	2.2	4.7	4×10^6	50	2×10^{23} IR	6
		38	5×10^5	50	6×10^{23} NH$_3$	6
W51–IRS 2	7.5	4	$\geq 10^7$	150	4.4×10^{24}	7
DR 21OH	3.0	12	$\geq 10^6$	150	2.2×10^{23} IR	8
					5.2×10^{23} molecules	8
NGC 7538	2.8	22	2×10^6	100	1.8×10^{24}	9
Ori(KL)	0.5	20	5×10^6	150	1.3×10^{24}	10
Sgr B2	10.0	(35)	2×10^5	90	$\sim 10^{24}$	11
W51M	7.5	20	2×10^5	120	10^{24}	12

NOTES.—(1) Wilson and Walmsley 1989. (2) Bally 1982. (3) Thronson *et al.* 1984; Mezger *et al.* 1988; Snell *et al.* 1984. The results give $A_v \sim 50$ or $N(H_2) \sim 10^{23}$ cm^{-2} for the warm dust at $T \sim 50$ K, and $A_v \sim 550$ or $N(H_2) \sim 10^{24}$ cm^{-2} for the cool dust plus protostellar condensation (Mezger *et al.* 1988). The two protostellar condensations in our beam (FIR Nos. 5, 6) are equivalent to two 8″ clumps. The density $n \sim 10^6$ cm^{-3} from CS studies (Snell *et al.* 1984). (4) Wootten, Loren, and Snell 1982. Distance and effective core size uncertain. Column density estimated from CO results (Turner 1987a). Effective core size estimated from $N(H_2)$ and an adopted distance of 1.5 kpc. (5) Density and T_k from Ziurys, Snell, and Dickman 1989. Uncertain distance (cf. DeNoyer 1977): 1.0 kpc adopted. See also White *et al.* 1987. (6) Density from Massi, Churchwell, and Felli 1988. This gives $N(H_2) = 6 \times 10^{23}$ cm^{-2} for each clump. By contrast, 50 μm IR has opacity $\gtrsim 0.4$ (Gatley *et al.* 1979), hence $A_v \sim 110$ mag, hence $N(H_2) \sim 2 \times 10^{23}$ cm^{-2}. This determination refers to interclump gas. (7) Bally *et al.* 1987. (8) Mangum, Wootten, and Mundy 1989; Harvey *et al.* 1986. The 100 μm opacity of 0.08 corresponds to $A_v = 123$ mag or $N(H_2) \sim 2 \times 10^{23}$ cm^{-2}, in reasonable agreement with the molecular value. (9) Pratap, Batrla, and Snyder 1990. (10) Nonmetastable NH$_3$ emission and 400 μm IR results (Genzel *et al.* 1982) both imply $n \sim 3 \times 10^7$ cm^{-3}, within the 6×10^{16} cm diameter of the core. We adopt physical conditions between those of the "outflow" and those of the hot core, namely, $n = 5 \times 10^6$ cm^{-3}, $T = 140$ K, $N(H_2) = 1.25 \times 10^{24}$ cm^{-2}. (11) Density and T_k from Cummins, Linke, and Thaddeus 1986 and Linke, Stark, and Frerking 1981. Core size and column density from Goldsmith *et al.* 1987. (12) Density and T_k from Andersson 1985. Column density from 400 μm IR results of Jaffe, Becklin, and Hildebrand 1984.

TABLE 5

PN ABUNDANCES IN WARM STAR-FORMING MOLECULAR CLOUD CORES

Source	T_R^* (mK)	θ_s (arcsec)	η_f	T_B (K)	Δv (km s^{-1})	X'	$N(PN)$	$X = N(PN)/N(H_2)$
				A. $J = 2$–1				
OMC-N	<50	25	0.091	<0.70	1.4	<7.2(−13)	<3.0(12)	<2(−11)
Ori B	≤20	2×8	0.019	≤1.3	2.2	<1.9(−12)	<1.2(13)	<4(−11)
NGC 2264	≤50	46?	0.39?	≤0.16	1.7	<4.6(−13)	<4.7(11)	<2(−12)
M17SW	31	4.7[a]	0.0032	12.2	5.2	2.0(−11)	3.1(14)	6.3(−10)
		38	0.23	0.17	5.2	8.8(−14)	6.9(11)	1.4(−12)
DR 21OH	31	12	0.021	1.87	4.8	4.8(−12)	6.9(13)	1.9(−10)
				B. $J = 5$–4				
NGC 2071	<80	~80	1.0	<0.17	3.8	<3.8(−12)	<4.3(12)	<7(−11)
IC 443C	<80	30	1.0	<0.17	~30	<1.9(−13)	<1.0(13)	<4(−11)
W51–IRS 2	≤80	4	0.010	≤17.0	5.1	≤1.4(−12)	<2.1(14)	<5(−11)
NGC 7538	~100	7.3[a]	0.034	6.26	8.0	1.5(−12)	7.2(13)	4.0(−11)
		22	0.39	0.55	8.0	1.2(−13)	5.8(12)	3.2(−12)
			C. Previously Observed PN Sources (only $J = 2$–1 Listed)					
Ori	23	20	0.058	0.50	12.7	1.2(−12)	2.3(14)	1.7(−10)
Sgr B2	44	30	0.13	0.43	18	9.2(−13)	5.0(13)	5.0(−11)
		7.5	0.0082	6.84	18	1.5(−11)	8.1(14)	8.1(−10)
W51M	20	20	0.058	0.435	11	8.0(−13)	1.1(13)	1.1(−11)
		1.4[a]	0.0003	88.7	11	8.0(−10)	2.6(16)	2.6(−8)

[a] Assumes 0.05 pc clumps (see text), for which $T_k = 100$ K, $n = 10^6$ cm^{-3} are adopted.

relate with the presence of detectable PN. Among sources with detectable PN, Ori(KL) and NGC 7538 are outflow regions but also contain nearby H II regions expanding into the dense molecular regions. By contrast, DR 21OH is a relatively "quiescent" massive star-forming region; the DR 21 H II region is 2.6 pc away and only represents an earlier star-forming episode along a north-south ridge that includes DR 21OH. Strong shocks may be inhibitory [cf. the 2000 K highly shocked region in Ori(KL)], and may explain the absence of PN in strong outflow regions such as W51–IRS 2 and NGC 2071, or in the supernova remnant IC 443. In addition to a strong outflow, NGC 2071 may also lack sufficient column depth. OMC-N and NGC 2264 may be too cool. Ori B should, however, be a likely candidate. In fact, there are hints of the $J = 2–1$ line in Ori B and NGC 2264 (denoted " $\lesssim$ " in Table 5).

All PN abundances derived in Table 5 are well below the values predicted by Millar, Bennett, and Herbst (1987) for ion-molecule chemistry, and together with the results of searches for other P compounds, discussed next, imply a large depletion factor for P $(10^3–10^4)$ in warm dense molecular clouds (§ Va).

IV. OTHER PHOSPHORUS COMPOUNDS

Existing chemical models for interstellar P compounds (Thorne et al. 1984; Millar, Bennett, and Herbst 1987) predict that, other than PN, the only other detectable species should be HPO. Additionally, it is fundamental to ion-molecule P chemistry that phosphine (PH_3) will not form. Finally, recent calculations by one of us (T. T.) indicate that under conditions of thermochemical equilibrium in the dense cores of CSEs, all phosphorus should be in the form of HCP. Accordingly, we describe results of searches for HPO, PH_3, and HCP.

a) HPO

Saito, Endo, and Hirota (1986) have identified HPO in the laboratory by its microwave spectrum and have established its molecular constants. HPO is an unstable asymmetric rotor with $\mu_a = 2.335$, $\mu_b = 0.51$ debye (Tapia, Allavena, and Lazilliere 1978). Small splittings of rotational levels with high K_{-1} quantum number are observed, owing to the phosphorus nuclear spin-rotation interaction. These splittings do not exceed 0.8 MHz for the transitions of relevance here, and will be ignored. The spectrum was calculated from the Saito et al. constants using a Watson A-reduced form of the Hamiltonian for centrifugal distortion.

Table 6 summarizes the observations of HPO. Lines appear at the calculated frequencies in the case of Sgr B2 $(5_{05}–4_{04})$ and
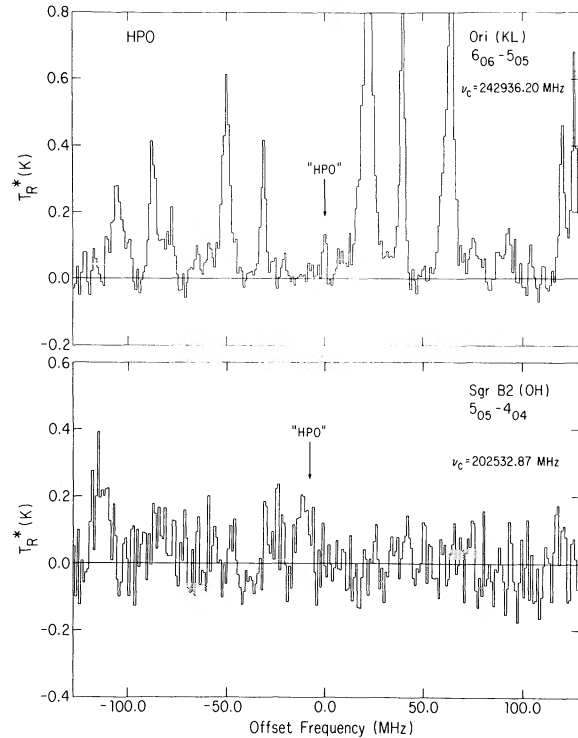

FIG. 2.—Spectra relevant to the HPO search. In neither of the sources shown can the observed feature be ascribed to HPO, because other transitions of HPO were not observed at expected intensities.

Ori(KL) $(6_{06}–5_{05})$, and are shown in Figure 2. An identification with HPO is not possible for Sgr B2 because there is no corresponding line at required strength at $6_{06}–5_{05}$ or at $2_{02}–1_{01}$. Similarly, we cannot identify HPO in Ori(KL) because of lack of an observed transition at $2_{02}–1_{01}$.

Because an accurate abundance ratio HPO/PN is required to test ion-molecule schemes for P compounds (§ Vc), we subject our negative results for HPO to an LVG radiation transfer analysis involving 46 energy levels, and using the same physical conditions for each source as were used to analyze PN (§ III). Collision cross sections for HPO are unknown. We have tested our results for a variety of cross sections ranging from pure dipole selection rules to pure "hard-sphere" collisions in which all ΔJ are equally likely. The range of HPO column densities is at most a factor of 3, depending on the cross sections. The adopted values correspond to cross sections

TABLE 6
OBSERVATIONS OF HPO

Transition	Frequency (MHz)	Source	T_R^* (mK)	Velocity Range (km s^{-1})	Resolution (km s^{-1})	Notes
$5_{05}–4_{04}$	202524.87	Sgr B2	200	62.0 ± 190	1.48	1
		W51M	<100	57.1 ± 190	1.48	
$6_{06}–5_{05}$	242936.23	Ori(KL)	100	9.0 ± 158	1.23	2
		Sgr B2	<80	62.0 ± 158	1.23	
		W51M	≲50	57.1 ± 158	1.23	
$6_{16}–5_{15}$	238311.39	Ori(KL)	<50	9.0 ± 161	1.26	
$2_{02}–1_{01}$	81069.61	Ori(KL)	<30	9.0	3.70	3
		Sgr B2	<30	62.0	3.70	3

NOTES.—(1) Line velocity = 70 km s^{-1}; HCOOH? (2) Line width = 2.5 km s^{-1}; EtCN? (3) Data from 3 mm survey of Turner 1989a.

TABLE 7

ABUNDANCE LIMITS FOR HPO

Source	Transition	T_R^* (mK)	θ_s (arcsec)	η_f	T_B^a (K)	Δv (km s^{-1})	T_k (K)	n (cm^{-3})	N(HPO) (cm^{-2})	N(HPO)/N(H$_2$)	N(HPC)/N(PN)
Ori(KL)	6_{06}–5_{05}	100	20	0.30	0.71	12.7	140	1(6)	...	...	...
	6_{16}–5_{15}	<50	...	0.30	<0.35	...	...	...	...	...	...
	2_{02}–1_{01}^{b}	<30	...	0.043	<0.82	...	...	...	<7.6(13)	<5(−11)	<0.3
SGR B2	5_{05}–4_{04}	200	30	1.0	0.42	...	...	...	...	...	...
	6_{06}–5_{05}	<80	...	1.0	<0.17	...	...	...	...	...	...
	2_{02}–1_{01}^{b}	<50	...	0.097	<0.61	18.0	50	1(6)	<4.7(13)	<5(−11)	<0.9
W51M	5_{05}–4_{04}^{b}	<100	20	0.30	<0.71	11.0	50	1(6)	<1.5(13)	<1(−10)	<15
	6_{06}–5_{05}	<50	...	0.30	≤0.35	...	...	...	...	...	...

^{a} At 240 GHz, $\eta_c = 0.47$ and $\theta_B = 33''$; at 81 GHz, $\eta_c = 0.84$ and $\theta_B = 80''$.

^{b} Transition providing the most sensitive abundance upper limits according to radiative transfer analysis.

inversely proportional to ΔJ and scaled for $\Delta J = 1$ to rates as calculated recently for HNCO by S. Green (1989, private communication; note that HNCO and HPO have similar quadrupole moments and therefore probably similar cross-section profiles). Our adopted cross sections are probably uncertain by no more than a factor of $\pm 50\%$, judging from the HNCO cross sections.

The HPO abundance results are collected in Table 7. In addition to the observations of HPO in the 202–243 GHz region, we have included the 2_{02}–1_{01} transition at 81069 MHz as observed in the 3 mm spectral survey of Turner (1989a). For a beamwidth of 80″ and $\eta_c \simeq 0.84$ at 81 GHz, our LVG results show that the 81 GHz transition permits considerably more sensitive limits to be placed on the HPO abundance than is possible using the higher frequency transitions, assuming a source size of 20″ or larger. The reason is that the HPO dipole moment ($\mu_a = 2.33$ debye) is large enough to inhibit significant population in levels as high as $J = 4$, even at densities as high as 10^6 cm^{-3}. Thus the W51M limits are noticeably less sensitive, since 81 GHz observations do not exist for this source.

b) PH$_3$

Phosphine is a symmetric top with a pyramidal structure similar to NH$_3$, but with negligible inversion splitting. The microwave spectrum and dipole moment ($\mu = 0.578$ debye) have been known for a long time (Helminger and Gordy 1969). Our present search of the 1_0–0_0 transition at 266944.52 MHz is considerably more sensitive than earlier ones, because our observed transition has 100 times the line strength and is at much lower energy than the weak $\Delta k = \pm 3$, $\Delta J = 0$ ($J = 6$ and $J = 8$) transitions searched by Hollis et al. (1980), and because the 12 m telescope has 6 times the collecting area of the MWO 4.9 m telescope used earlier by Loren and Wootten (1984) to search Ori(KL) at 267 GHz.

Unfortunately, the 1_0–0_0 transition of PH$_3$ is within 2 MHz of the (30, 9, 21)–(31, 8, 24) transition of SO$_2$ (266943.15 MHz; energy 42.6 cm^{-1} above ground) and about 7 MHz from the (15, 4, 12)–(15, 2, 13) transition of EtCN (266951.64 MHz; 39.3 cm^{-1} above ground). Thus it is not surprising that in highly energetic sources such as Ori(KL) and W51M we have detected emission lying close to the PH$_3$ transition but which we identify as SO$_2$. Figure 3 shows the spectra toward these sources. In Ori(KL) the observed line corresponds to SO$_2$ at a velocity of 9.0 km s^{-1}, as expected for the "plateau" component (Schloerb et al. 1983). The line width (12 km s^{-1}) appears considerably narrower than is usual for SO$_2$ (~ 30 km s^{-1}), but our signal-to-noise ratio is not sufficient to state this definitely. SO$_2$ transitions of higher energy than the present

one have been detected in Ori(KL), so there is little doubt that the observed line is SO$_2$. Similar statements are true for W51M, where in addition to SO$_2$ the EtCN line at 266952 MHz is seen. These species therefore restrict the upper limits attainable for PH$_3$. These transitions of SO$_2$ and EtCN are not observed in Sgr B2, so that more sensitive PH$_3$ limits are established. Our failure to detect PH$_3$ in interstellar sources is consistent with ion-molecule chemistry for P (§ Vb). Our failure to detect PH$_3$ in IRC 10216 is also not surprising. Although NH$_3$ is seen in both the outer envelope (Nguyen-Q-Rieu et al. 1984) and the inner core of IRC 10216, it is believed to originate under thermochemical equilibrium conditions in the inner core. Under such conditions, the dominant P compound is expected to be HCP rather than PH$_3$ (§ Vc).

Our results are analyzed with an LVG radiative transfer model, using collision rate coefficients for NH$_3$ as calculated
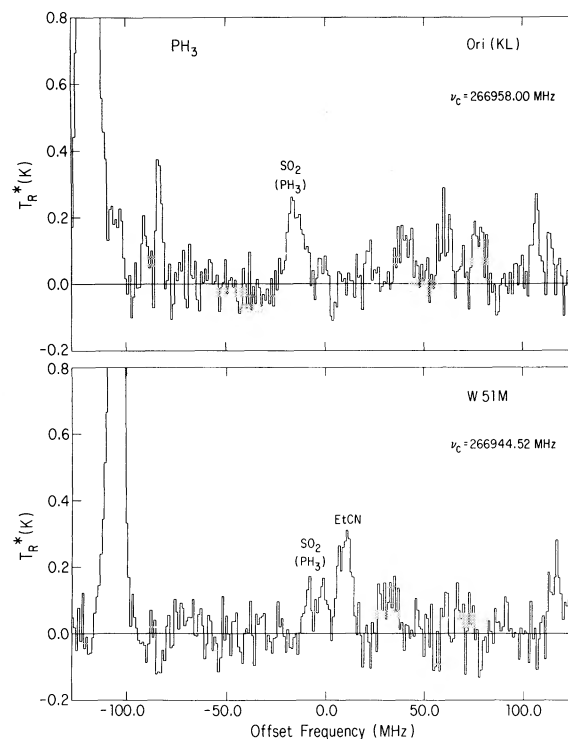

FIG. 3.—Spectra relevant to the PH$_3$ search. PH$_3$ at 266944.52 MHz is confused by the (30, 9, 21)–(31, 8, 24) transition of SO$_2$ (266943.15 MHz), which lies 42.6 cm^{-1} above ground. The SO$_2$ line imposes effective upper limits on PH$_3$.

TABLE 8

OBSERVATIONS AND ANALYSIS OF PH_3[a]

Sources	T_R^* (K)	θ_s (arcsec)	η_f	T_B^b (K)	Δv^c (km s^{-1})	T_k (K)	n (cm^{-3})	$N(PH_3)^d$ (cm^{-2})	$N(PH_3)/N(H_2)$	PH_3/PN
Ori(KL)	≤0.24[a]	20	0.39	≤1.62	12.0	150	1(6)	≤6(14)	≤5(−10)	≤3
Sgr B2	<0.10	30	1.0	<0.26	18.0	50	1(6)	<2(14)	<2(−10)	≤4
W51M	≤0.15[a]	20	0.39	≤1.0	10.0	50	1(6)	≤2(14)	≤2(−10)	≤15
IRC 10216	<0.08	...	...	...	...	...	...	...	...	...

[a] 1_0–0_0 transition at 266944.52 MHz. Contaminated by SO_2 [(30, 9, 21)–(31, 8, 24) at 266943.15 MHz] and possibly by EtCN [(15, 4, 12)–(15, 2, 13) at 266951.64 MHz], which limit the achievable sensitivity.

[b] At 267 GHz, $\eta_c = 0.38$, $\theta_B = 30''$.

[c] Spectral resolution is 1.12 km s^{-1} (1 MHz) for all data.

[d] $N(PH_3) = (4/3)N_{ortho}(PH_3)$ is assumed; N_{ortho} is calculated by LVG radiative transfer model, including nine ortho levels and NH_3 cross sections (see text).

by Danby et al. (1988). Because the observed PH_3 transition involves ortho–PH_3, and because ortho and para forms do not interconvert by radiative or collisional transitions, we have analyzed only the ortho form. Nine energy levels, involving energies as high as 200 K, are included. B, D_J, and D_{JK} constants were taken from Helminger and Gordy (1969), and the C constant (PH_3 is an oblate symmetric top) from Huber and Herzberg (1979). Appropriate sum rules are applied in converting the collision rate coefficients for NH_3, which has resolved inversion splitting, into appropriate rate coefficients for PH_3, whose inversion splitting is unresolved. The ortho/para abundance ratio of PH_3 is assumed to be the ratio of statistical weights (3:1), so that the total PH_3 abundance is 4/3 times the derived ortho abundance.

Observations and derived results for PH_3 are collected in Table 8.

c) HCP

The microwave spectrum of the linear species HCP has been measured by Johns, Stone, and Winnewisser (1971). The dipole moment is small, 0.3 debye. The quadrupole splitting arising from the spin-1 P atom is also smaller than in the analogous HCN molecule, and is of no consequence at millimeter wavelengths.

Table 9 lists the observations of HCP. HCP is clearly not detected in Sgr B2 or W51M. In Ori(KL) a line corresponding to $J = 6$-5 is seen at a velocity of 5 km s^{-1} (the hot-core velocity), but there is insufficient confirming evidence at either the $J = 5$-4 transition (confusion with EtCN) or at the $J = 7$-6 transition (inadequate sensitivity) to claim HCP. This is particularly true, since the observed line width of the feature at 239.694 GHz is somewhat narrower than typical hot-core line widths (10–15 km s^{-1}).

HCP has been searched for in IRC 10216 using both the NRAO 12 m and the IRAM 30 m telescopes. Although the 12 m results suggest a detection of both the $J = 6$-5 (20 mK) and $J = 5$-4 (60 mK) transitions, the 30 m results indicate at best a hint of the $J = 4$-3 and $J = 6$-5 transitions. The 30 m results are shown in Figure 4, and were adopted for our analysis, since they are more sensitive for a small source like IRC 10216. We interpret the 30 m results as upper limits.

We have analyzed the HCP results for IRC 10216 with an LVG radiative transfer model suitable for an expanding CSE observed with a Gaussian beam, as described by Morris (1975) and by Kuiper et al. (1976). Both intensity and profile shapes are fitted. Assumed parameters are a mass-loss rate of 9×10^{-5} $M_\odot$ yr^{-1}, an inner shell radius of $35R_* = 2 \times 10^{15}$ cm, a maximum shell expansion velocity of 14.0 km s^{-1}, a turbulent velocity component of 1 km s^{-1}, and a distance of 290 pc for IRC 10216. A power-law dependence is adopted for the rotational excitation temperature: $T_{rot} = 200 \ r^{-0.64}$ (Bieging, Chapman, and Welch 1984). The fractional abun-

TABLE 9

OBSERVATIONS OF HCP

Transition	Frequency (MHz)	Source	T_R^* (mK)	v_{LSR} (km s^{-1})	Resolution (km s^{-1})	Δv (km s^{-1})	θ_s (arcsec)	η_f	T_B^a (K)
$J = 4$-3	159802.56	IRC 10216[b]	≲50[c]	26.0	1.88	26	...	...	...
$J = 5$-4	199749.42	Ori(KL)	<250[d]	9.0	1.50	...	20	0.185	<2.37
		IRC 10216[b]	≤70	−26.0	3.00	30	...	...	...
$J = 6$-5	239693.82	Ori(KL)	<30	9.0	1.25	...	20	0.255	<0.25
			70	5.0	1.25	6.3	20	0.255	0.584
		IRC 10216[b]	≲29	−26.0	1.25	27	...	...	...
			≲40[c]	−26	1.25	27	...	...	...
		Sgr B2	<30	62.0	1.25	...	30	1.0	<0.064
		W51M	<40	57.1	1.25	...	20	0.255	<0.334
$J = 7$-6	279634.66	Ori(KL)	<100	9.0	1.07	...	20	0.476	<0.60
		IRC 10216[b]	<30	−26.0	2.15	...	...	...	...
		Sgr B2	<100	62.0	1.07	...	30	1.0	<0.286
		W51M	<100	57.1	1.07	...	20	0.476	<0.60

[a] Values of η_c for the NRAO 12 m telescope are 0.57, 0.47, and 0.36 at 200, 240, and 280 GHz. θ_B is 40″, 33″, and 28″, respectively. For the IRAM 30 m, $T_R \equiv T_{MB} = 1.67T_A^*$ and $\theta_B = 17''$ at 160 GHz; $T_{MB} = 2.0T_A^*$ and $\theta_B = 14''$ at 240 GHz.

[b] See text and Table 10 for expanding-shell LVG models of IRC 10216, and for choices of θ_s. T_B varies across source for optically thin lines.

[c] Observed with the IRAM 30 m telescope.

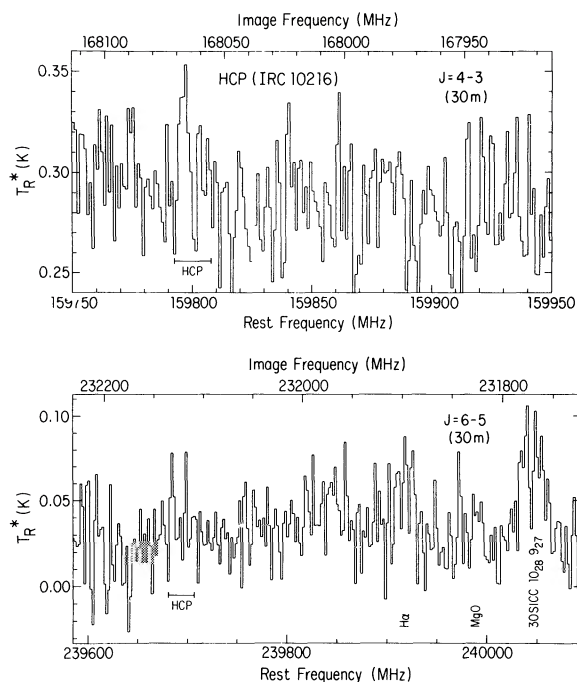[d] Confused with EtCN [(12, 2, 10)–(11, 1, 11) at 199751.50 MHz].

Fig. 4.—HCP in IRC 10216, as observed with the IRAM 30 m telescope. There are hints of the $J = 4$–3 and $J = 6$–5 transitions which are consistent with the expected abundance of HCP as deduced (§ Vd) from the abundance of the recently detected CP and from our thermochemical equilibrium models (§ Vd).

dance, outer shell radius, and antenna beam size are nominal free parameters.

There are two important considerations in the analysis of HCP for IRC 10216:

1. CP has recently been detected in IRC 10216 (Guelin et al. 1989). The CP line profiles are flat-topped, implying that the source size is smaller than the 12″ observing beam. The abundance ratio is [CP]/[P] $\simeq$ 0.04.

2. In § Vc we show that under thermochemical equilibrium conditions all gas-phase P is in the form HCP. Thus $X(\mathrm{HCP}) = 2.7 \times 10^{-7}$, the adopted abundance of P, in the inner envelope.

It is of interest to compare the CP results with those of interferometric observations of HCN (Bieging, Chapman, and Welch 1984) and SiS (Bieging and Nguyen-Q-Rieu 1989) as well as recent IRAM 30 m observations of AlF and AlCl, which show them to be slightly extended relative to the 14″ observing beam. Thus:

HCN dissociates to CN at $r = 6″$; CN is extended throughout the envelope.
HCP dissociates to CP at $r < 6″$; CP disappears at $r \approx 6″$.
SiS dissociates at $r \approx 12″$.
AlF, AlCl have not dissociated at $r \approx 6″$.

We expect polyatomic species to dissociate more easily than diatomics, and covalent bonded diatomics (SiS) more easily than ionic-bonded diatomics (AlF, AlCl). These expectations are consistent with the observations. The two questions of interest are: (1) What happens to the CP in the outer envelope? (2) What is the photodissociation radius of HCP?

We analyze three cases for HCP in IRC 10216:

1. We investigate how efficiently HCP photodissociates to CP (or condenses onto grains) after outflowing from the inner

core. Thus we ask what source size (θ_s) will produce the observed upper limit to the 30 m antenna temperature. We find $\theta_s \leq 2″1$ (8.9×10^{15} cm), assuming a constant value of $X(\mathrm{HCP})$ over the source size. In reality, depletion of HCP would not occur suddenly at a radius of θ_s. More realistic models, using $X = X_0 r^{-\beta}$ with $X_0 = 2.7 \times 10^{-7}$ and $\beta \sim 1$, yield an effective size at which $X(\mathrm{HCP})$ has decreased to $0.5X_0$. This effective size is $\lesssim 2″5$. Grains are thought to be fully condensed at a radius $r \simeq 2″4$ (10^{16} cm). These values allow the possibility that virtually all HCP condenses onto grains, with perhaps 4% remaining free to form CP at 4% of the P abundance. However, it is not obvious that HCP should condense much more efficiently than HCN, which appears to remain largely in the gas phase.

2. If HCP does not adsorb efficiently onto grains, then some HCP may survive out to radii characteristic of HCN (6″) or even SiS (12″). Accordingly, we fix the source size θ_s for HCP at larger values and ask what fractional abundance X_0, taken as constant with r, produces the observed upper limits. Values of $\theta_s = 6″$, 9″, 12″, and 15″ produce values of $X_0 = 5 \times 10^{-8}$, 3.5×10^{-8}, 2.5×10^{-8}, and 2.5×10^{-8}, corresponding to HCP/P = 0.18, 0.13, 0.09, and 0.09, respectively. These results allow the possibility that 80%–90% of HCP has adsorbed onto grains, while another 4% has dissociated to CP, leaving $\sim 5\%$ of HCP in the gas phase, which is just below our detection level. In these models, HCP transition opacities are very much less than unity.

3. The HCP source radius is fixed at 6″, the HCN source size, and X_0 is fixed at the predicted value of 2.7×10^{-7}. We find that a value 0.9 of the exponent β is needed in the power law $X = X_0 r^\beta$ to explain the upper limit of observed antenna temperature.

The interstellar sources have been analyzed with the LVG radiative transfer model suitable for a homogeneous spherical cloud. Eight energy levels are included, and cross sections for HCN are used. The assumed physical conditions and resulting abundances are given in Table 10.

V. THE CHEMISTRY OF PHOSPHORUS COMPOUNDS

a) PN

Unlike Si, P is not significantly depleted in the diffuse ISM. Relative to the cosmic abundance of 3.2×10^{-7}, Dufton, Keenan, and Hibbert (1986) find no depletion of P in warm diffuse clouds, and a depletion of a factor of 3 in cold diffuse clouds. The fate of P in dense molecular clouds is, however, unknown.

The possibility that significant quantities of P may remain in the gas phase in dense clouds prompted Thorne, Anicich, and Huntress (1983) and Thorne et al. (1984) to study the gas-phase chemistry of P in the laboratory. P chemistry is found to differ significantly from that of N, the first-row analog. Unlike NH_n^+ ions, PH_n^+ ions react endothermically with H_2, so that PH_n compounds ($n = 1$–3) are very unlikely at low temperatures. Based on the limited number of reactions studied, Thorne et al. (1984) predicted that species containing the P—O bond should dominate, because P^+ and PH^+ react readily with H_2O, which is highly abundant in an oxygen-rich gas. $H_3O^+ + P$ also contributes. Under typical dense molecular cloud conditions ($n = 10^5$ cm^{-3}), Thorne et al. (1984) predicted that 85% of the available phosphorus remains in atomic form, 14% resides in PO, and 1% exists in all other P species. In particular, species containing P—N and P—C bonds are predicted to be rare

TABLE 10

ABUNDANCES FOR HCP[a]

A. INTERSTELLAR SOURCES

Source	T_R^* (K)	Δv^{b} (km s^{-1})	θ_s (arcsec)	T_B (K)	T_k (K)	n (cm^{-3})	$N(\mathrm{HCP})^{\mathrm{c}}$ (cm^{-2})	$N(\mathrm{HCP})/N(\mathrm{H_2})$	HCP/PN
Ori(KL)	≤70	12.7	20	≤0.58	150	1(6)	≤5.3(14)	≤4.4(−10)	≤2.6
Sgr B2	<30	18	30	<0.064	50	1(6)	<1.1(14)	<1.1(−10)	<2.2
W51M	<40	11	20	<0.33	50	1(6)	<3.5(14)	<3.5(−10)	<32

B. IRC 10216

Case	T_R^* (mK)	Δv (km s^{-1})	θ_s (arcsec)	β^{d}	X_0^{e}
Model 1: 30 m	≤40	28	≤2.1	0	2.7(−7)
Model 2: 30 m	≤40	28	6.0	0	5.0(−8)
	≤40	28	12.0	0	2.5(−8)
Model 3: 30 m	≤40	28	6.0	0.9	2.7(−7)

[a] All calculations are based on the $J = 6$–5 transition, which gives the most sensitive abundance limit.

[b] Assumed for purposes of analysis, based on PN line widths.

[c] $N = X'n\Delta v$.

[d] Defined as $X = X_0(r/r_0)^{-\beta}$ with $r_0 = 2 \times 10^{15}$ cm.

[e] Fractional abundance calculated for the inner (undepleted) core; for models 1 and 3, X_0 is taken as the TE value of 2.7(−7).

because they require reaction of P$^+$ or PH$^+$ with NH$_3$ or CH$_4$, which are much less abundant than H$_2$O.

The detection of PN at an abundance level $\sim 10^{-10}$ (Turner and Bally 1987; Ziurys 1987), coupled with the upper limits of 1.5×10^{-11} established for PO by Matthews, Feldman, and Bernath (1987), indicated a major deficiency in the Thorne *et al.* (1984) picture. Millar, Bennett, and Herbst (1987) recognized the possibility of the reaction PO + N → PN + O as an explanation of the observed PN/PO discrepancy. Incorporation of this reaction, and several others such as PO + N → P + NO, PH + N → PN + H, and PN + N → N$_2$ + P, into the chemical networks used by Millar, Leung, and Herbst (1987), leads to predictions of 77%, 20%, and 2.3% of available gas-phase phosphorus in the form of P, PN, and HPO, respectively, under steady state conditions. Similar abundances are predicted for early-times models. To reproduce the observed abundance of PN in Ori(KL), Millar, Bennett, and Herbst (1987) require a depletion factor of 1000 for phosphorus.

i) *Lack of* PN *in Cold Clouds: Implications*

Fractional abundances of PN are at least 10 times less in several cold cloud cores ($T_k \sim 10$ K) than in warm star-forming regions such as Ori(KL), and in the case of TMC-1, at least 100 times less (Table 4).

There are several explanations for this result in terms of the Millar, Bennett, and Herbst (1987) model.

1. The reaction PO + N → PN + O may have an activation energy. This possibility is regarded by Millar, Bennett, and Herbst (1987) as unlikely, on the grounds that the analogous reaction NO + N → N$_2$ + O, which is the dominant formation path for N$_2$ in dense clouds, is known to proceed without an activation barrier. If an activation barrier does exist, then PO would become the dominant form of phosphorus. Unfortunately, PO was not searched for by Matthews, Feldman, and Bernath (1987) in cold cloud cores, so this possibility is not disproved observationally.

2. The overall reaction rate for PO + N → (PN + O,

P + NO) may be much smaller than the value of 3.4×10^{-11} cm^3 s^{-1} adopted at $T = 50$ K by Millar, Bennett, and Herbst (1987) by analogy with the rate of the NO + N reaction. Radical-radical or radical-atom neutral reactions which lack activation barriers have a $T^{0.5}$ temperature dependence (Prasad and Huntress 1980). Therefore, the overall rate of PO + N may be ~ 2.2 times smaller in cold clouds than the adopted value, but such a reduction should be of no consequence, since model tests by Millar, Bennett, and Herbst (1987) yield a calculated PN abundance which is insensitive to the overall rate so long as it exceeds $\sim 5 \times 10^{-13}$ cm^3 s^{-1}. Also, for rates less than this, the predicted PO abundance is much greater than observed upper limits.

3. The branching ratio for the PO + N → PN + O reaction is taken as $\frac{1}{4}$ by Millar, Bennett, and Herbst (1987) who find that the PN abundance would fall below observed values in warm sources only if the branching ratio is less than ~ 0.01. Note that PO + N → PN + O is exothermic by 0.21 eV, while PO + N → P + NO is exothermic by 0.34 eV, so a branching ratio as low as 0.01 is unlikely. In any case, an unexpectedly low branching ratio affects the predicted PN abundance, and hence the predicted depletion of phosphorus, but does not explain a lower abundance in cold clouds, since branching ratios are not expected to be T-dependent.

4. PN might be destroyed more efficiently in cold clouds than in warm ones by reactions not considered by Millar, Bennett, and Herbst (1987). Reactions of PN with H$_3^+$, HCO$^+$, and H$_3$O$^+$ (species more abundant in cold clouds than in warm clouds) are shown by Millar, Bennett, and Herbst (1987) simply to recycle back to PN rather than destroy it. The reaction PN + N → N$_2$ + P does not recycle back to PN, but this reaction is expected to have an activation energy and thus result in more, rather than less, PN in cold clouds. In general, any neutral-neutral reaction which might destroy PN should be slower, not faster, in cold clouds.

5. The depletion of P in cold dense clouds is greater than in warm dense clouds. With adopted values as described above, Millar, Bennett, and Herbst (1987) require a depletion factor of

10^3 to explain the observed PN abundance in Ori(KL) and other warm clouds, and thus factors of at least 10^5 are needed to explain the PN upper limit in TMC-1.

Only possibilities 1 and 5 appear viable to explain the 100-fold or greater decrease in PN in cold clouds. Of these, possibility 5 appears much the likelier because, unless the Millar, Bennett, and Herbst (1987) model is seriously in error, it already requires a large P-depletion factor to explain the observed PN abundance in warm clouds. In addition, PN is observed only in highly energetic star-forming regions where shocks and outflows could disrupt grains and release (a small fraction of the) phosphorus. As pointed out by Turner and Bally (1987), the observation that SiO/Si $\sim$ PN/P ($\sim 4 \times 10^{-4}$) seems to be more than a coincidence. Our conclusion is that these fractions indicate roughly the depletion of both Si and P by a factor of order 10^3. Once 10^{-3} of the cosmic abundance of Si and P is released from the grains in star-forming regions, a relatively large fraction of the gas-phase Si and P forms SiO and PN, respectively (cf. the recent study of Si gas-phase chemistry by Herbst et al. 1989). In cold clouds, virtually all Si and P must remain locked in grains. Our PN results imply a P-depletion factor greater than 10^5 in TMC-1, while recent upper limits for SiO of 2×10^{-12} (Ziurys, Snell, and Dickman 1989) indicate an Si-depletion factor greater than 10^6.

ii) Warm Clouds

The nominal PN abundance of 10^{-10}, taken in the context of the Millar, Bennett, and Herbst (1987) model, implies a depletion factor of 10^3 for phosphorus in Ori(KL) and other star-forming molecular clouds. As discussed in § III, the PN abundance is quite uncertain, however. The range of derived PN abundances (Table 5) is nominally 3×10^{-12} to 8×10^{-10}, but under extreme assumptions (a $1\rlap{.}''4$ source size for W51M) it could be as high as 2.6×10^{-8}. The latter value would imply that P is essentially undepleted (by a factor of ~ 2) if 20% of all P forms PN.

If P is really locked into grains in all but the most energetic conditions, it is of interest to compare it with Si, both to test this general hypothesis and to see whether there are significant differences between Si and P under grain-disrupting conditions. We consider Ori(KL) the best-understood energetic source.

For the high-velocity flow source (the "plateau" source from which PN seems to arise), Wright et al. (1983) find an interferometrically determined SiO source size of $15'' \times 30''$, and estimate $n = 10^6$ cm^{-3}, $T_k = 230$ K, $\Delta v = 20$ km s^{-1}. Using these parameters, the analysis of Turner and Steimle (1985) gives $N(\text{SiO}) = 2.2 \times 10^{15}$ cm^{-2}, or SiO/Si $= 5.6 \times 10^{-4}$. The recent models of Herbst et al. (1989) show that 97.5% of all available Si forms SiO under these conditions. Therefore, a depletion factor for Si of ~ 1750 is implied, to be compared with a depletion factor of 1000 for PN.

For completeness, we consider the unlikely case that PN arises in the hot core (the observed line profiles indicate that this is not the case). In this case, using a source size of $5'' \times 10''$ (Wright et al. 1983), $n = 10^7$ cm^{-3}, $T_k = 230$ K, and $\Delta v = 20$ km s^{-1}, Turner and Steimle (1985) found that $X(\text{SiO}) = 3.4 \times 10^{-7}$, or SiO/Si $= 1.2 \times 10^{-2}$. The Si-depletion factor is then 85. By reducing the PN source size from $20''$ (Table 5) to that of SiO and using $n = 10^7$ cm^{-3}, we find $X(\text{PN}) = 1.3 \times 10^{-9}$. If 20% of all P forms PN, the depletion factor for P is 50, again comparable to that of Si, but much smaller than for the plateau source.

One other comparison, that of sulfur, may be made among second-row elements. Using abundances as determined for Ori(KL) by Johansson et al. (1984), we find (SO + SO$_2$ + CS + OCS)/S $= 1.8 \times 10^{-2}$. If all available S forms only these compounds, a depletion factor of 55 is implied for S. When other S species, such as H$_2$CS, HCS$^+$, SiS, and H$_2$S, are included, the depletion factor for S would be smaller. S compounds appear to originate mostly in the plateau source, and Si, P compounds only in the plateau source. However, there is overlap between hot-core and plateau components in observed line profiles, and a small fraction of these species could arise in the hot core. Therefore, a detailed comparison of the relative depletions is unwarranted. The best comparison is for P and Si in the plateau source. In general, we can conclude only that all second-row elements are significantly depleted even under energetic conditions near star formation.

Although virtually all Si and P are locked up in grains in cold cloud cores, the situation is less clear for sulfur. "Normal" fractional abundances of CS, OCS, and SO might seem to imply that most sulfur is free, but at least one model (Prasad and Huntress 1982) requires a significant depletion of sulfur in order to explain the abundances of CS and SO. The large observed abundances of C$_2$S, C$_3$S, and H$_2$CS (one or two orders of magnitude above predicted ion-molecule values if sulfur is undepleted) would then be inconsistent with their production by reactions of S$^+$ with C$_2$H$_2$, as suggested by Smith et al. (1988). Interstellar sulfur chemistry thus continues to be poorly understood, so that conclusions about S depletion in cold versus hot regions are unwarranted.

b) PH$_3$

It seems clear that phosphine, PH$_3$, is difficult to synthesize by ion-molecule reactions in interstellar clouds. Since none of the PH$_n^+$ ($n = 0$–4) ions react with H$_2$ to form new P—H bonds, there is no sequence of reactions to saturate the P$^+$ ion with H atoms as there is in the case of N$^+$ and O$^+$. PH$^+$ forms via P + XH$_n^+$ $\to$ PH$^+$, but PH$^+$ reacts rapidly to form P—O or other heteratom bonds. PH forms via several dissociative recombination reactions involving HPO$^+$, HPN$^+$, and H$_2$PO$^+$, but PH is quickly removed by PH + N $\to$ PN + H. Thus the slow pathway PH + XH$^+$ $\to$ PH$_2^+$, ..., followed by PH$_4^+$ + metal $\to$ PH$_3$, would not produce significant quantities of PH$_3$. The simple model of Thorne et al. (1984) predicts PH$_3$/P $< 3 \times 10^{-5}$, while the more extensive model of Millar, Bennett, and Herbst (1987) finds PH$_3$/P $< 5 \times 10^{-4}$ and PH$_3$/PN $< 2 \times 10^{-3}$.

Our observed limits for PH$_3$/PN exceed unity in all sources, and thus are consistent with, but do not constrain, the expected ion-molecule chemistry.

If grains require disruption (e.g., by strong shocks) to produce gas-phase P, it is possible that the densities and temperatures may be high enough to permit thermochemical equilibrium (TE) chemistry of the highly refractory elements in which endothermic reactions may proceed. At 600 K, however, our TE calculations (§ Vc) for a C-rich environment show that PH$_3$ comprises only a fraction 10^{-10} of the total phosphorus, decreasing to 10^{-13} at $T = 1000$ K. For O-rich (interstellar) environments, the fractions are 4×10^{-11} and 10^{-13}, respectively. Thus our modest upper limits for the PH$_3$ abundance provide no constraints on the possibility of TE chemistry in energetic interstellar sources.

While all gas-phase chemistries predict negligible abundances of PH$_3$, it is possible that PH$_3$ might form efficiently on grain surfaces, where, as in the case of NH$_3$, simple hydro-

PHOSPHORUS IN DENSE ISM

genation processes are believed efficient (e.g., Brown, Charnley, and Millar 1988). This might particularly apply to the P-PH_3 case, since ion-molecule reactions leave most phosphorus in the atomic form in the gas phase. The large abundance of NH_3 observed in several star-forming cores is thought to result from the evaporation of the grain mantles in which NH_3 is the dominant repository of nitrogen. The failure to detect PH_3 then implies one of the following: (1) PH_3 does not form on grain surfaces, analogous to NH_3; (2) in contrast to NH_3, PH_3 is not easily evaporated (at ~ 90 K); (3) the evaporated PH_3 reacts to form another P compound. We consider the second possibility unlikely, since all grain mantle molecules are thought to be trapped in a dominant H_2O ice matrix, and hence all are expected to evaporate at the sublimation temperature for H_2O (90 K). The third scenario is also unlikely, since at 90 K a stable molecule such as PH_3 in a $^1A_1$ ground state is depleted only by ion-molecule reactions. Reaction of PH_3 with H_3^+ or HCO^+ likely recycles back to PH_3. C^+ is the dominant destruction agent for PH_3, but the C^+ abundance is very low in dense cores, and must be a negligible depletion agent just as it is for NH_3 in regions where NH_3 is rapidly evaporated from grains. We conclude that the first explanation is most likely, not only by process of elimination but also because the much higher depletion of P than of N in dense clouds indicates a very different chemistry for these two species on grains.

c) HPO

Our observations have shown that HPO/PN < 0.3 in Ori(KL), with less stringent limits in the other sources (Table 7). The Millar, Bennett, and Herbst (1987) model predicts HPO/PN = 0.12 for steady state, 0.014 for early times. HPO is formed via $(H_3^+, HCO^+) + P \rightarrow PH^+$ followed by $PH^+ + H_2O \rightarrow HPO^+ + H_2$, $H_2PO^+ + H$, and finally $H_2PO^+ + e \rightarrow HPO$, PO. The intermediate reaction is measured (Thorne et al. 1984) to favor HPO^+ over H_2PO^+ by 2.4 to 1. Dissociative recombination of HPO^+ leads to PO and PH, while Millar, Bennett, and Herbst (1987) assume that most H_2PO^+ leads to HPO (cf. Bates 1986), with small amounts of PO and PH also formed.

Our upper limits for HPO constrain the range of depletion possible for P. Millar, Bennett, and Herbst (1987) argued that the reaction $PN + N \rightarrow N_2 + P$, if active at low temperatures (it has a probable activation barrier), would reduce the predicted PN abundance, and thus the nominal observed PN abundance of 10^{-10} could be explained by a depletion factor as low as 10, rather than the large value of 10^3 as otherwise derived for the Ori plateau source. Any attempt to reduce the P-depletion factor will, however, increase the predicted HPO abundance proportionately, unless appropriate additional destructive reactions for HPO exist which are not included in the model. Under steady state, the depletion factor for P can be reduced from 10^3 to no lower than 400 without increasing the predicted HPO/PN abundance ratio above our observed limit. Thus our HPO limit is additional evidence that the P depletion is high, and is comparable to that of Si.

d) HCP

i) Interstellar Sources

According to the models (Thorne et al. 1984; Millar, Bennett, and Herbst 1987), HCP is not expected to be produced in significant quantity by ion-molecule chemistry. Forma-

tion mechanisms are $P^+ + CH_4 \rightarrow HCPH^+ + H_2$ and $P + CH_3^+ \rightarrow HCPH^+ + H$, with the second process dominating because $P/P^+ \sim 10^3$ in dense interstellar clouds. However, the low abundance of CH_3^+ compared with H_3O^+ means that $HCP/PO \ll 1$ is expected. Indeed, the models predict $HCP/H_2 < 10^{-14}$, much below our observed upper limit of 10^{-10} (Table 10).

ii) Thermochemical Equilibrium Models: IRC 10216

Of the seven heavy elements now identified in interstellar and circumstellar molecules, P turns out to be unique in one important aspect: the compounds that it forms under TE conditions are completely different from those formed by ion-molecule processes. We have established this by carrying out TE models of the type performed by Tsuji (1973, 1987), for CSEs, but now including phosphorus in more detail. The C-rich case (C > O) is considered here. The model includes 36 elements and 240 molecules, since it is relevant mostly to the CSE context. Equilibrium constants are evaluated for the molecules using either molecular constants given in the JANAF thermochemical tables or constants as used in previous models (Tsuji 1973). The results for P compounds are shown in Figure 5. The total gas pressure is $\log P_g = -3.0$ and P/H is taken as 2.7×10^{-7}. Calculations were performed over the range $600 \le T \le 2000$ K in 200 K steps.

The results show that all phosphorus is contained in the form HCP for all temperatures believed relevant to C-rich CSEs. Thus we expect a fractional abundance $X(HCP) = 2.7 \times 10^{-7}$ within the inner zone of IRC 10216 where TE applies.

The size of the inner TE region is uncertain: it certainly includes the photosphere of the central star and may persist to a radius of $\sim 10^{14}$ cm (2–3 stellar radii). Dust condensation appears to begin at a radius of 8–10 R_* ($\sim 5 \times 10^{14}$ cm), and the dust density appears to vary as r^{-2}. Dust formation is thought to continue out to a radius of $\sim 10^{16}$ cm (2″.4).

Although P compounds appear to be highly depleted in interstellar sources, the conditions of high temperatures and of large velocity differences between gas and dust in the inner envelope of IRC 10216 have been argued to inhibit depletion
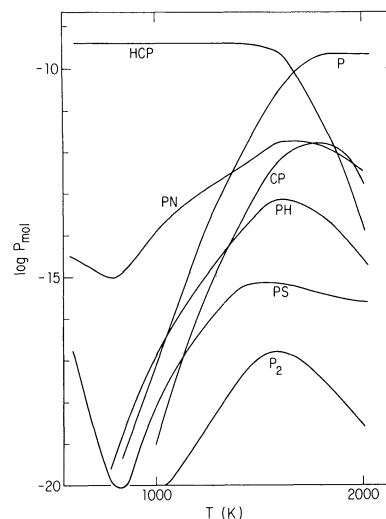

FIG. 5.—Thermochemical equilibrium model results for P compounds for a C-rich environment with $\log P_g = -3.0$. All phosphorus resides in the form HCP for temperatures of relevance to C-rich CSEs.

onto grains (Jura and Morris 1985). In § VIc we found for three distinct models that HCP must be severely depleted, at least by the time it reaches the likely photodissociation radius of 6″, and quite possibly at the radius of 2″.4 at which grain formation is complete. The constraint that CP/P $\simeq$ 0.04 means that no more than 4% of HCP need survive in the gas phase at the photodissociation radius, if photodissociation to CP is efficient. Note that CN/N $\approx$ 0.03 (Guelin et al. 1989), so that one might conclude that HCN adsorbs onto grains at least as efficiently as HCP. However, CN is located in the outermost envelope, while CP itself is somehow depleted at much smaller radii. It is therefore unwarranted to draw conclusions about HCP versus HCN from observations of CP and CN. While nitrogen is not believed to condense onto grains inside $r = 2″.5$, phosphorus is expected to form the refractory high-temperature condensate Fe_3P (Fegley and Lewis 1980), and since the cosmic abundance ratio Fe/P $\gg$ 3, this may tie up most or all of the P.

It is of interest to compare these conclusions for P compounds with those for Si species in IRC 10216. SiO and SiS together incorporate all of the gas-phase Si under TE conditions, for $T \lesssim 800$ K (Tsuji 1987). Observationally, Morris et al. (1979) find SiO/Si $\lesssim 0.01$ and SiS/Si $\lesssim 0.04$ in the outer envelope. The implication is that either these Si compounds are almost entirely accreted onto grains, or else gas-phase Si itself is largely condensed, presumably into silicate form (e.g., $MgSiO_3$) inside $r = 2″.4$ (10^{16} cm). While the line profiles for SiO and SiS make it clear that the lines are formed mainly in the outer envelope, it is not clear at what radii the bulk of the Si material is depleted. SiC_2 is also seen in the outer envelope, but is likely formed by ion-molecule reactions between Si^+ and C_2H_2. The Si^+ could arise from photodestruction of SiS or SiO, and thus does not indicate that any gas-phase Si survives into the outer envelope. The alkali metal compounds (NaCl, KCl, AlCl, AlF) have observed abundances (Cernicharo and Guelin 1987b) between 25 and 1000 times lower than predicted by TE models (Tsuji 1973; cf. the review by Turner 1989b), while cusped line profiles and limited mapping of AlF and AlCl (Lucas and Guelin 1989) show that at least the Al species persist at low abundances into the outer envelope. Thus most Al, Na, and K appears likely to have condensed in the inner core. These circumstances make it likely that P compounds (HCP and CP) survive at low abundances into the outer envelope, and we expect that HCP itself should be detectable at a level just below the limit we have established here.

VI. DEPLETIONS OF FIRST- AND SECOND-ROW ELEMENTS: A SUMMARY

In Table 11 we collect current information on the depletions [in terms of log (X/X_{solar})] of first- and second-row elements. First-row elements, as well as sulfur, are seen to be only modestly depleted, even in dense clouds, and there is no evidence that their depletions increase significantly with higher densities. These are the so-called volatile elements. By contrast, Mg, P, Si, and Ca exhibit large depletions in dense clouds, and Si and Ca also have significant depletions in the diffuse ISM. Based on optical information, P appears to be little depleted at low densities, and is often considered a volatile element. Our present work shows that it is highly refractory, at least in dense clouds.

Nitrogen, oxygen, and sulfur are expected to be little depleted in the ISM, because their main condensation products (NH_3, H_2O, H_2S) are highly volatile. Although N, O, and S atoms are chemisorbed on silicate or other grain surfaces, under modest densities they react with atomic H on the grain surfaces to form their volatile hydrides. These are easily photodesorbed or evaporated near star-forming regions. Once in the gas phase, they are easily photodissociated, or destroyed by shocks. Perhaps 25% of O will be locked up in refractory silicate grains. Thus N, O, and S should be largely undepleted in the diffuse ISM, and remain largely in the gas phase in dense clouds as well, although in the form of molecules. The observation of many compounds of N, O, and S even in cold dense clouds supports these general ideas, although the mechanism of desorption remains obscure in such sources.

Carbon is somewhat more depleted in general. One possible reason is that solid carbon is the thermodynamically favored phase at high densities and temperatures such as occur in the outflows of evolved stars. Another is that C can form large molecules that can be resistive to photodestruction and which can be locked up in grains (the so-called organic refractory dust component; see Tielens and Allamandola 1987).

In this paper we have presented evidence that P and Si are highly depleted in all dense clouds, warm or cold. Neither element is highly depleted in the diffuse ISM. To explain the latter, Tielens and Allamandola (1987) have suggested that both Si and P, when accreted onto grains, form saturated volatile hydrides (SiH_4, PH_3) which are easily photodesorbed and photodissociated in the diffuse ISM. This suggestion does not explain why P and Si are noticeably more depleted in diffuse

TABLE 11

ELEMENTAL DEPLETIONS (log X/X_{solar})

Cloud Type	log n	N	O	C	S	Mg	P	Si	Ca
Diffuse (warm)	-1.5[a]	-0.12	-0.39	...	~ 0	-0.2	-0.09	-0.6	-1.2
Diffuse (cold)	0.5[a]	-0.12	-0.39	-0.51	...	-0.71	-0.73	-1.6	-3.6
Dense (warm)	≥ 5	-0.2?[b]	-0.4?[b]	-0.5?[b]	~ -1.7	?	-3[c]	-3.2[d,e]	?
Dense (cold)	≥ 4	-0.2?[b]	-0.4?[b]	-0.5?[b]	-1.7?[f]	?	≤ -5[c]	≤ -7.2[d]	?

[a] From Jenkins 1987.
[b] Values adopted in most chemical models, which are reasonably successful in explaining observed molecular abundances.
[c] This work.
[d] Deduced using the model of Herbst et al. 1989.
[e] Turner and Steimle 1985.
[f] Dense (warm) cloud value guesstimated, since observed abundances of S compounds are comparable; however, fewer S species are presently detected in dense cold clouds.

clouds than N, O, and S (Table 11), for which Tielens and Allamandola apply the same argument.

It is highly unlikely that (silicate) grains *condense* in the ISM (as distinct from accreting; see Turner 1989b and references therein). Such grains very likely originate in the outflows of evolved stars, where they were created under TE conditions. Under TE at high temperatures, Si can form $MgSiO_3$ and P can form Fe_3P, both refractory high-T condensates (Tielens and Allamandola 1987). Given the cosmic abundances of the constituent elements, most of the Si and Mg can be locked up in $MgSiO_3$, and most of the P in either Fe_3P or in adsorbed HCP. Our analysis of the observed molecules of these elements suggested that this is indeed the case in IRC 10216 (§ Vd). Thus, although the dominant gas-phased molecules SiO, SiS, HCP, CP, and PS (in O-rich CSEs) will be easily photodissociated in the diffuse ISM outside the CSEs, their small abundances cannot account for the modest depletion observed for Si and P in the diffuse ISM.

To explain the observed properties of Si and P, we suggest that evolved stellar outflows contain Si solely in the form of $MgSiO_3$ (SiO is observed to be negligible), and P in the form of Fe_3P and adsorbed HCP. Some $MgSiO_3/Fe_3P$ grain cores survive passage through the diffuse ISM, possibly because they are coated with refractory organic mantles before being expelled from CSEs. These mantles, followed by the cores themselves, are eroded away by photoprocessing on a time scale of less than $\sim 4 \times 10^8$ yr (Greenberg 1987), unless they enter a "dense" cloud, where they are protected. Thus the modest depletions of Si and P in diffuse clouds indicate the almost total erosion of grain cores in such clouds, whose extinctions do not offer sufficient protection. In such clouds, Si and P form the volatile saturated species SiH_4 and PH_3 on grain surfaces. These compounds are easily photodesorbed and dissociated, so there are equilibrium abundance ratios SiH_4/Si and PH_3/P that depend on the extinction. When these species enter dense clouds (or the diffuse cloud evolves into a dense cloud), these ratios will become large, and the hydrides will reside on grain surfaces. Any residual gas-phase Si will form SiO via ion-molecule reactions (Herbst *et al.* 1989), and any residual gas-phase P will form PN. The binding energy of SiO onto grain surfaces (or, equivalently, the condensation temperature) is very large, 29,500 K (Jura and Morris 1985). Thus there is no possibility of desorption of the SiO except under highly energetic conditions. The expected depletion of Si under such conditions depends on several factors (sticking probability, i.e., incident velocity, grain composition, etc.). Jura and Morris (1985) estimate large depletion factors for SiO in IRC 10216 despite the large outflow velocities. Large depletion factors may be expected for dense interstellar clouds as well.

The low depletion of P in diffuse clouds (lower than Si) suggests that the dominant TE forms of P in CSEs (HCP, PS) either escape into the ISM in gas phase, where they are photodissociated, or that they are not strongly adsorbed onto grains and are subsequently photodesorbed and photodissociated. Our limits on the HCP abundance appear to rule out the former possibility. Similarly, we find it implausible that the condensed form Fe_3P would photoerode more efficiently than $MgSiO_3$, especially if both have protective organic mantles. The most likely possibility, that P is largely in the form of HCP adsorbed onto grains, explains both the observed modest depletion of P in the diffuse ISM and also our failure to detect HCP in IRC 10216.

In dense clouds, our cold cloud results indicate that the PN

formed from the residual gas-phase P must become firmly adsorbed into grains, just as does SiO. This will occur after only a short time ($\sim 10^4$ yr at $n = 10^6$ cm^{-3}). While condensation temperatures are not available in the literature for PN or other P compounds, some general considerations may be applied. The binding energy under van der Waals–type interactions is proportional to the product of the polarizabilities of the adsorbed and surface species. Polar molecules have much stronger binding than nonpolar species. Thus species such as N_2, CO, O_2, and CH_4 are weakly bound and highly volatile (Leger, Jura, and Omont 1985). These species are highly abundant and may evaporate from surfaces at temperatures as low as ~ 15 K, thus ensuring that the first-row elements N, O, and C are not strongly depleted even in cold dense clouds. Polar species such as NH_3 and H_2O are much more refractory, and require special processes such as spot heating by cosmic rays or chemical explosions to be desorbed in cold dense clouds (Leger, Jura, and Omont 1985). There is ample observational evidence that these species are evaporated in large quantities when grains are heated to $\gtrsim 90$ K in star-forming regions such as Ori(KL). With their large dipole moments of 2.75 and 2.4 debye, PN and HPO can be expected to be strongly bound. Assuming that the earlier-adsorbed PH_3 is also strongly bound, a high depletion of P can be expected in dense clouds, as we have deduced. On this simple picture, PN and HPO must be much more strongly bound than NH_3 and H_2O. It should be emphasized that binding energies are not always related simply to molecular dipole moments. For example, H_2S and C_2H_2 have very similar binding energies (despite C_2H_2 being nonpolar), which are intermediate between the volatiles (N_2, CO, O_2, CH_4) and the more refractory species (HCN, NH_3, H_2O). The dominant gas-phase S species is OCS (Herbst and Leung 1989), whose small dipole moment (0.7 debye) might explain the fact that S seems only modestly depleted in dense clouds.

Our study of phosphorus compounds is consistent with ion-molecule models of P chemistry. Because only one compound dominates the gas-phase chemistry of both P (PN) and Si (SiO), it is possible to estimate the depletions of these elements in dense clouds with fewer uncertainties than for other elements. Even under energetic conditions near star-forming regions, the depletion of P and Si remains high ($> 10^3$), suggesting that grains are not appreciably disrupted where these molecules occur. It is unclear just how these species are adsorbed and desorbed, but they probably reside in grain mantles, since a disruption of the grain cores themselves would imply little or no depletion, contrary to observation.

VII. SUMMARY AND CONCLUSIONS

Our principal observational results are the following:

1. PN has been detected in several additional star-forming regions. The abundance is difficult to determine, owing to uncertainties in physical conditions (mainly source size), and may range from 4×10^{-11} to 2×10^{-8}. The preferred value is 2×10^{-10}, based on the best-understood sources Ori(KL) and DR 21OH. PN is not detected in cold clouds, with limits at least 100 times below those of star-forming regions.

2. HPO and PH_3 are not detected. PH_3 is not expected. HPO is expected at levels comparable to or slightly below our upper limits.

3. HCP is not detected (or expected) in interstellar sources, nor yet in IRC 10216, where it is expected on the basis of

thermochemical equilibrium models if it is not depleted on grains.

On the basis of an improved understanding of ion-molecule chemistry of second-row elements (P: Thorne *et al.* 1984, Millar, Bennett, and Herbst 1987; Si: Herbst *et al.* 1989), and of thermochemical equilibrium chemistry of P (developed in this paper), we conclude the following from our observational results:

1. Phosphorus is depleted by factors of 10^3 in dense star-forming cores, and by more than 10^5 in cold cloud cores. This conclusion is based mainly on our PN results, but a small ambiguity in the PN chemistry is removed by our upper limits on HPO.

2. TE conditions do not occur, or are unimportant, in star-forming regions, as shown by the lack of HCP.

3. In IRC 10216, depletion of HCP onto grains is indicated, as is found also for Si and alkali metal compounds. Some HCP survives out to the photodissociation radius of 6″, as is the case

for Si and alkali metal compounds, and is photodissociated to CP, recently detected by Guelin *et al.* (1989). Neither gas-phase HCP nor CP can explain the observed low depletion of interstellar P in diffuse regions. If the HCP is essentially all combined onto grains in the inner core, which we consider likely, then the adsorption is modeled to be complete essentially at the outer radius of dust formation.

We have proposed an overall picture of circumstellar and interstellar grain and gas-phase processes to explain the depletions of both first- and second-row elements, and in particular the high depletions of Si and P in dense clouds. On this picture, no further Si molecules are likely to be detected in interstellar clouds, and only HPO remains to be detected among phosphorus species. We suggest that the depletion properties of Mg will be similar to those of Si in dense clouds, and thus that gas-phase Mg will be detectable in molecular form, once its ion-molecule chemistry is understood, and assuming that only one or two molecular species dominate its chemistry.

REFERENCES

Andersson, M. 1985, in *Proc. ESO Workshop 22, Millimeter and Submillimeter Astronomy* (Aspenas, Sweden) (Garching: ESO), p. 353.
Avery, L. W., MacLeod, J. M., and Broton, N. W. 1982, *Ap. J.*, **254**, 116.
Bally, J. 1982, *Ap. J.*, **261**, 558.
Bally, J., Arons, J. F., Ball, R., Becker, R., and Lacy, J. 1987, *Ap. J. (Letters)*, **323**, L73.
Bates, D. R. 1986, *Ap. J. (Letters)*, **306**, L45.
Benson, P. J., and Myers, P. C. 1989, *Ap. J. Suppl.*, **71**, 89.
Bieging, J. H., Chapman, B., and Welch, W. J. 1984, *Ap. J.*, **285**, 656.
Bieging, J. H., and Nguyen-Q-Rieu, 1989, *Ap. J. (Letters)*, **343**, L25.
Brown, P. D., Charnley, S. B., and Millar, T. J. 1988, *M.N.R.A.S.*, **231**, 409.
Campbell, B., and Thompson, R. I. 1984, *Ap. J.*, **279**, 650.
Cernicharo, J., and Guelin, M. 1987a, *Astr. Ap.*, **176**, 299.
————. 1987b, *Astr. Ap.*, **183**, L10.
Cummins, S. A., Linke, R. A., and Thaddeus, P. 1986, *Ap. J. Suppl.*, **60**, 819.
Danby, G., Flower, D. R., Valiron, P., Schilke, P., and Walmsley, C. M. 1988, *M.N.R.A.S.*, **235**, 229.
DeNoyer, L. K. 1977, *Ap. J.*, **212**, 416.
Dufton, P. L., Keenan, F. P., and Hibbert, A. 1986, *Astr. Ap.*, **164**, 179.
Fegley, B., and Lewis, J. S. 1980, *Icarus*, **41**, 439.
Gatley, I., Becklin, E. E., Sellgren, K., and Werner, M. W. 1979, *Ap. J.*, **233**, 575.
Genzel, R., Downes, D., Ho, P. T. P., and Bieging, J. 1982, *Ap. J. (Letters)*, **259**, L103.
Gerin, M., Wootten, H. A., Combes, F., Boulanger, F., Peters, W. L., Kuiper, T. B. H., Encrenaz, P. J., and Bogey, M. 1987, *Astr. Ap.*, **173**, L1.
Goldsmith, P. F., Snell, R. L., Hasagawa, T., and Ulkita, N. 1987, *Ap. J.*, **314**, 525.
Greenberg, J. M. 1987, in *IAU Symposium 120, Astrochemistry*, ed. M. S. Vardya and S. P. Tarafdar (Dordrecht: Reidel), p. 501.
Guelin, M., Cernicharo, J., Paubert, G., and Turner, B. E. 1990, *Astr. Ap.*, **230**, L9.
Harris, A., Townes, C. H., Matsakis, D. N., and Palmer, P. 1983, *Ap. J. (Letters)*, **265**, L63.
Harvey, P. M., Campbell, M. F., and Hoffman, W. F. 1977, *Ap. J.*, **211**, 786.
Harvey, P. M., Joy, M., Lester, D. F., and Wilking, B. A. 1986, *Ap. J.*, **300**, 737.
Helminger, P., and Gordy, W. 1969, *Phys. Rev.*, **188**, 100.
Herbst, E., and Leung, C. M. 1989, *Ap. J. Suppl.*, **69**, 271.
Herbst, E., Millar, T. J., Wlodek, S., and Bohme, D. K. 1989, *Astr. Ap.*, **222**, 205.
Hollis, J. M., Snyder, L. E., Lovas, F. J., and Ulich, B. L. 1980, *Ap. J.*, **241**, 158.
Huber, K. P., and Herzberg, G. 1979, *Molecular Spectra and Molecular Structure. IV. Constants of Diatomic Molecules* (New York: Van Nostrand).
Jaffe, D. T., Becklin, E. E., and Hildebrand, R. H. 1984, *Ap. J. (Letters)*, **279**, L51.
Jenkins, E. B. 1987, in *Interstellar Processes*, ed. D. J. Hollenbach and H. A. Thronson (Dordrecht: Reidel), p. 533.
Johansson, L. E. B., *et al.* 1984, *Astr. Ap.*, **130**, 227.
Johns, J. W. C., Stone, J. M. R., and Winnewisser, G. 1971, *J. Molec. Spectrosc.*, **38**, 437.
Jura, M., and Morris, M. 1985, *Ap. J.*, **292**, 487.
Kuiper, T. B. H., Knapp, G. R., Knapp, S. L., and Brown, R. L. 1976, *Ap. J.*, **204**, 408.
Leger, A., Jura, M., and Omont, A. 1985, *Astr. Ap.*, **144**, 147.
Lichten, S. M. 1982, *Ap. J.*, **253**, 593.
Linke, R. A., and Goldsmith, P. F. 1980, *Ap. J.*, **235**, 437.
Linke, R. A., Stark, A. A., and Frerking, M. A. 1981, *Ap. J.*, **243**, 147.
Loren, R. B., and Wootten, H. A. 1984, unpublished MWO result.
————. 1986, *Ap. J.*, **306**, 142.
Lucas, R., and Guelin, M. 1990, in *Submillimeter Astronomy*, ed. G. D. Watt and A. S. Webster (Dordrecht: Kluwer), p. 97.

Madden, S. C., Irvine, W. M., Matthews, H. E., Friberg, P., and Swade, D. A. 1989, *A.J.*, **97**, 1403.
Mangum, J. G., Wootten, H. A., and Mundy, L. G. 1988, in *Submillimeter Astronomy*, ed. G. D. Watt and A. S. Webster (Dordrecht: Kluwer), p. 185.
————. 1989, private communication.
Massi, M., Churchwell, E., and Felli, M. 1988, *Astr. Ap.*, **194**, 116.
Matthews, H. E., Bell, M. B., and Feldman, P. A. 1988, unpublished.
Matthews, H. E., Feldman, P. A., and Bernath, P. F. 1987, *Ap. J.*, **312**, 358.
Mauersberger, R., Henkel, C., and Wilson, T. L. 1987, *Astr. Ap.*, **173**, 352.
Mauersberger, R., Henkel, C., Wilson, T. L., and Walmsley, C. M. 1986, *Astr. Ap.*, **162**, 199.
Mezger, P. G., Chini, R., Kreysa, E., Wink, J. E., and Salter, C. J. 1988, *Astr. Ap.*, **191**, 44.
Millar, T. J., Bennett, A., and Herbst, E. 1987, *M.N.R.A.S.*, **229**, 41P.
Millar, T. J., Leung, C. M., and Herbst, E. 1987, *Astr. Ap.*, **183**, 109.
Morris, M. 1975, *Ap. J.*, **197**, 603.
Morris, M., Redman, R., Reid, M. J., and Dickinson, D. F. 1979, *Ap. J.*, **229**, 257.
Mundy, L. G. 1984, Ph.D. thesis, University of Texas, Austin.
Mundy, L. G., Snell, R. L., Evans, N. J., Goldsmith, P. F., and Bally, J. 1986, *Ap. J.*, **306**, 670.
Myers, P. C., Linke, R. A., and Benson, P. J. 1983, *Ap. J.*, **264**, 517.
Nguyen-Q-Rieu, Graham, D., and Bujarnabal, V. 1984, *Astr. Ap.*, **138**, L5.
Persson, S. E., Geballe, T. R., Simon, T., Lonsdale, C. J., and Baas, F. 1981, *Ap. J. (Letters)*, **251**, L85.
Prasad, S. S., and Huntress, W. T. 1980, *Ap. J. Suppl.*, **43**, 1.
————. 1982, *Ap. J.*, **260**, 590.
Pratap, P., Batrla, W., and Snyder, L. E. 1990, *Ap. J.*, **351**, 530.
Saito, S., Endo, Y., and Hirota, E. 1986, *J. Chem. Phys.*, **84**, 1157.
Schloerb, F. P., Friberg, P., Hjalmarsson, A., Hoglund, B., and Irvine, W. M. 1983, *Ap. J.*, **264**, 161.
Scoville, N. Z., Sargent, A. I., Sanders, D. B., Claussen, M. J., Masson, C. R., Lo, K. Y., and Phillips, T. G. 1986, *Ap. J.*, **303**, 416.
Seab, C. J. 1987, in *Interstellar Processes* ed. D. J. Hollenbach and H. A. Thronson (Dordrecht: Reidel), p. 491.
Smith, D., Adams, N. G., Giles, K., and Herbst, E. 1988, *Astr. Ap.*, **200**, 191.
Snell, R. L., and Bally, J. 1986, *Ap. J.*, **303**, 683.
Snell, R. L., Scoville, N. Z., Sanders, D. B., and Erickson, N. R. 1984, *Ap. J.*, **284**, 176.
Stutzki, J., Stacey, G. J., Genzel, R., Harris, A. L., Jaffe, D. T., and Lugten, J. B. 1988, *Ap. J.*, **332**, 379.
Swade, D. A. 1987, Ph.D. thesis, University of Massachusetts.
Swade, D. A., and Schloerb, F. P. 1987, in *Interstellar Matter: A Symposium in Honor of A. H. Barrett*, ed. J. M. Moran and P. T. P. Ho (New York: Gordon & Breach), p. 183.
Takano, T., Fukui, Y., Ogawa, H., Takaba, H., Kawabe, R., Fujimoto, Y., Sugitani, K., and Fujimoto, M. 1984, *Ap. J. (Letters)*, **282**, L69.
Tapia, O., Allavena, M., and Lazilliere, M. 1978, *Chem. Phys. Letters*, **56**, 25.
Thorne, L. R., Anicich, V. G., and Huntress, W. Y. 1983, *Chem. Phys. Letters*, **98**, 162.
Thorne, L. R., Anicich, V. G., Prasad, S. S., and Huntress, W. T. 1984, *Ap. J.*, **280**, 139.
Thronson, H. A., Lada, C. J., Schwartz, P. R., Smith, H. A., Smith, J., Glaccum, W., Harper, D. A., and Lowenstein, R. F. 1984, *Ap. J.*, **280**, 154.
Tielens, A. G. G. M., and Allamandola, L. J. 1987, in *Interstellar Processes*, ed. D. J. Hollenbach and H. A. Thronson (Dordrecht: Reidel), p. 397.
Tsuji, T. 1973, *Astr. Ap.*, **23**, 411.
————. 1987, in *IAU Symposium 120, Astrochemistry*, ed. M. S. Vardya and S. P. Tarafdar (Dordrecht: Reidel), p. 409.

Turner, B. E. 1989a, *Ap. J. Suppl.*, **70**, 539.
———. 1989b, *Space Sci. Rev.*, **51**, 235.
Turner, B. E., and Bally, J. 1987, *Ap. J.* (*Letters*), **321**, L75.
Turner, B. E., and Steimle, T. C. 1985, *Ap. J.*, **299**, 956.
White, G. J., Rainey, R., Hayashi, S. S., and Kaifu, N. 1987, *Astr. Ap.*, **173**, 337.
Wilson, T. L., and Walmsley, C. M. 1989, *Astr. Ap. Rev.*, in press.
Wootten, H. A., and Loren, R. B. 1987, *Ap. J.*, **317**, 220.

Wootten, H. A., Loren, R. B., and Snell, R. L. 1982, *Ap. J.*, **255**, 160.
Wootten, H. A., Snell, R. L., and Evans, N. J. 1980, *Ap. J.*, **240**, 532.
Wright, M. C. M., Plambeck, R. L., Vogel, S. N., Ho, P. T. P., and Welch, W. J. 1983, *Ap. J.* (*Letters*), **267**, L41.
Ziurys, L. M. 1987, *Ap. J.* (*Letters*), **321**, L81.
Ziurys, L. M., Snell, R. L., and Dickman, R. L. 1989, *Ap. J.*, **341**, 857.

J. BALLY: AT&T Bell Laboratories, HOH L-245, Holmdel, NJ　07733

J. CERNICHARO: IRAM, Avenida Divina Pastora, 7 NC, E-18012 Granada, Spain

M. GUELIN: IRAM, Domaine Universitaire de Grenoble, Voie 10, F-38406, St. Martin d'Hères, France

T. TSUJI: Tokyo Astronomical Observatory, Mitaka, Tokyo 181, Japan

B. E. TURNER: NRAO, Edgemont Road, Charlottesville, VA　22903